Lecture 4

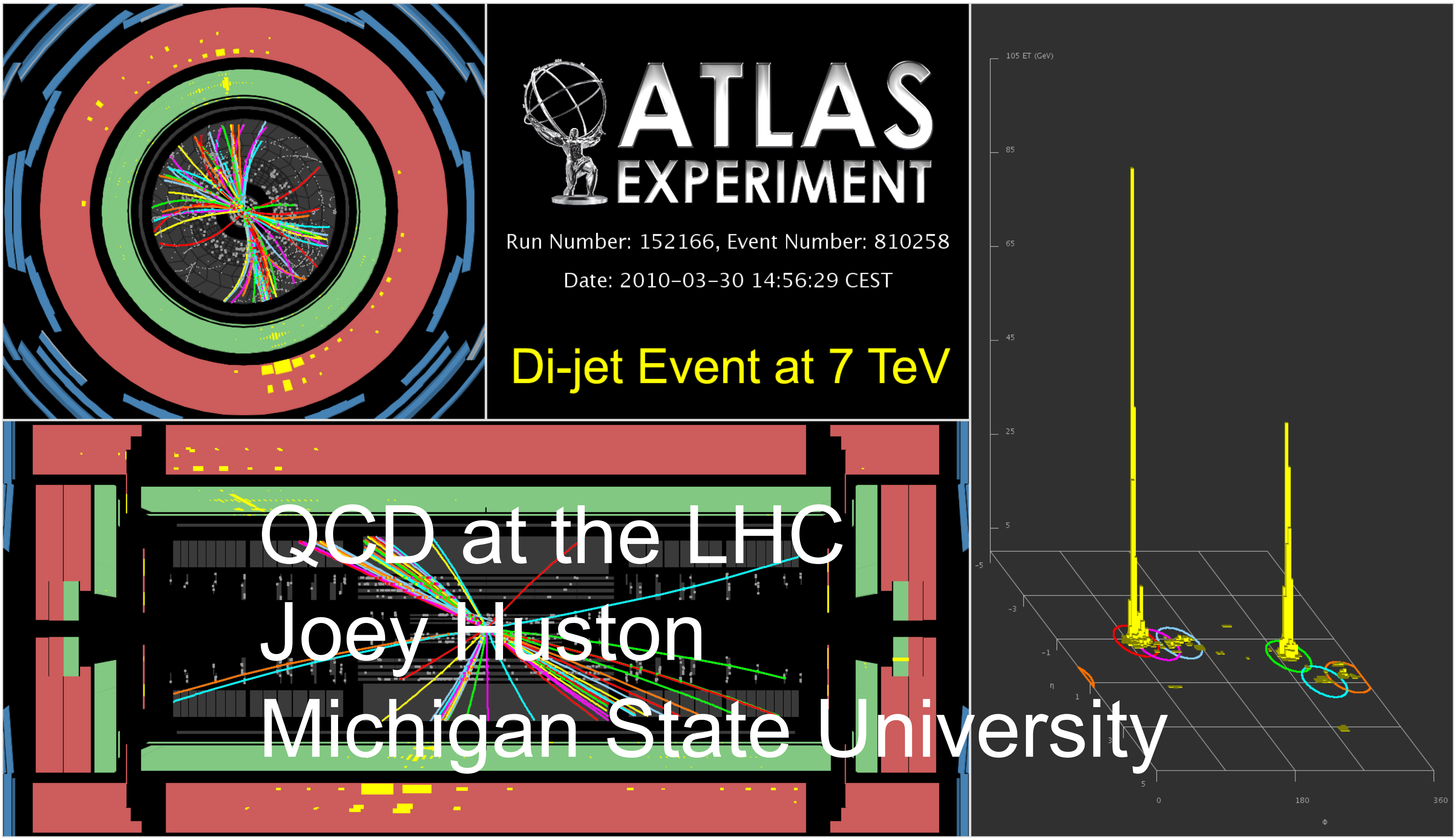

QCD at the LHC

Joey Huston
Michigan State University

A question from Eric

- Why do the low number eigenvectors correspond to the best determined directions?
- These are the directions in which the χ^2 function increases most steeply if you vary the parameters from the their central fit values

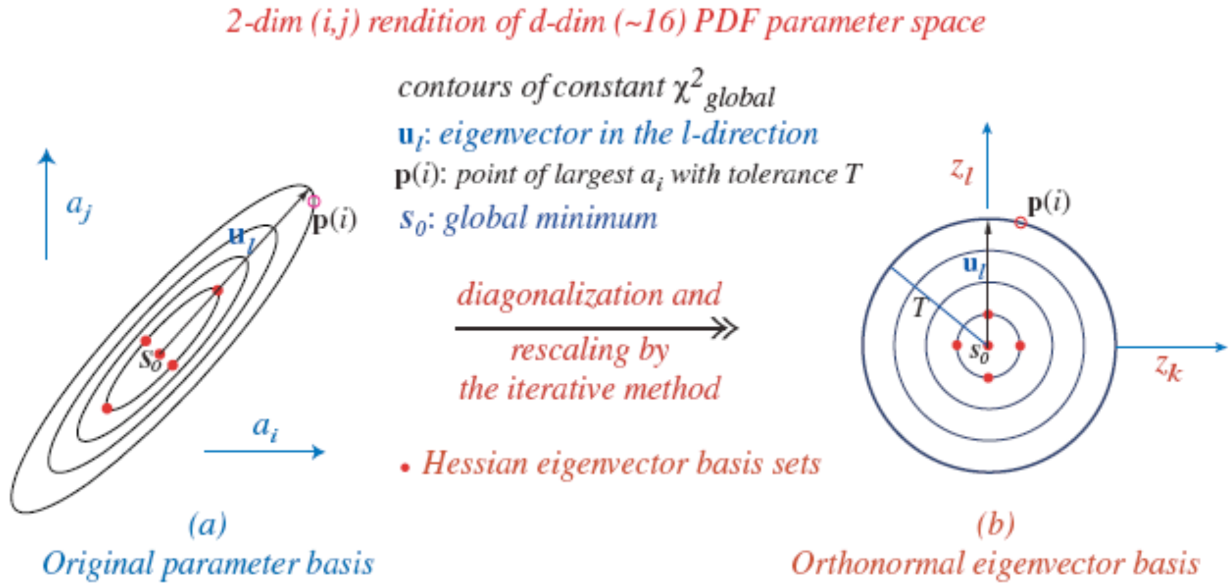

Figure 28. A schematic representation of the transformation from the pdf parameter basis to the orthonormal eigenvector basis.

- Finishing up on PDFs

My recommendation to PDF4LHC/Higgs working group

- Cross sections should be calculated with MSTW2008, CTEQ6.6 and NNPDF
- Upper range of prediction should be given by upper limit of error prediction using prescription for combining α_s uncertainty with error PDFs
  - in quadrature for CTEQ6.6 and NNPDF
  - using eigenvector sets for different values of α_s for MSTW2008
  - (my suggestion) as standard, use 90%CL limits
  - note that this effectively creates a larger α_s uncertainty range
- Ditto for lower limit
- So for a Higgs mass of 120 GeV at 14 TeV,it turns out that the gg cross section lower limit would be defined by the CTEQ6.6 lower limit (PDF+α_s error) and the upper limit defined by the MSTW2008 upper limit (PDF+α_s error)
  - with the difference between the central values primarily due to α_s
  - I'll come back to using the Higgs as an example in the last lecture
- To fully understand similarities/differences of cross sections/uncertainties conduct a benchmarking exercise, to which all groups are invited to participate
- To be discussed in lecture #5

NNLO addendum

- NNLO is important for some cross sections (as we saw for gg->Higgs)
- Not all processes used for global fits are available at NNLO (inclusive jet production for example)
- Only global fit at NNLO currently is MSTW
- Current paradigm is to apply NLO uncertainty band to NNLO predictions from MSTW
  - basically a factor of 2 increase over MSTW errors by themselves
- Most of NNLO corrections for Higgs production are from matrix element rather than differences in PDFs between NLO and NNLO
- So K factor (NNLO/LO) can also be used to some reasonable approximation

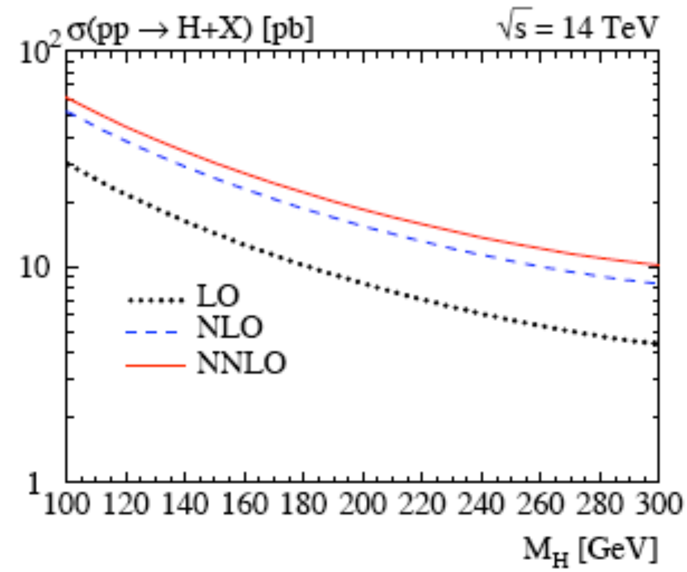

For CTEQ: α_s series

- Take CTEQ6.6 as base, and vary $\alpha_s(m_Z)$ +/-0.002 (in 0.001 steps) around central value of 0.118
- Blue is the PDF uncertainty from eigenvectors; green is the uncertainty in the gluon from varying α_s
- We have found that change in gluon due to α_s error (+/-0.002 range) is typically smaller than PDF uncertainty with a small correlation with PDF uncertainty over this range
  - as shown for gluon distribution on right
- **PDF error and α_s error can be added in quadrature**
  - expected because of small correlation
  - in recent CTEQ paper, it has been proven this is correct regardless of correlation, within quadratic approximation to χ^2 distribution

arXiv:1004.4624; PDFs available from LHAPDF

So the CTEQ prescription for calculating the total uncertainty (PDF+α_s) involves the use of the 45 CTEQ6.6 PDFs and the two extreme α_s error PDF's (0.116 and 0.120)

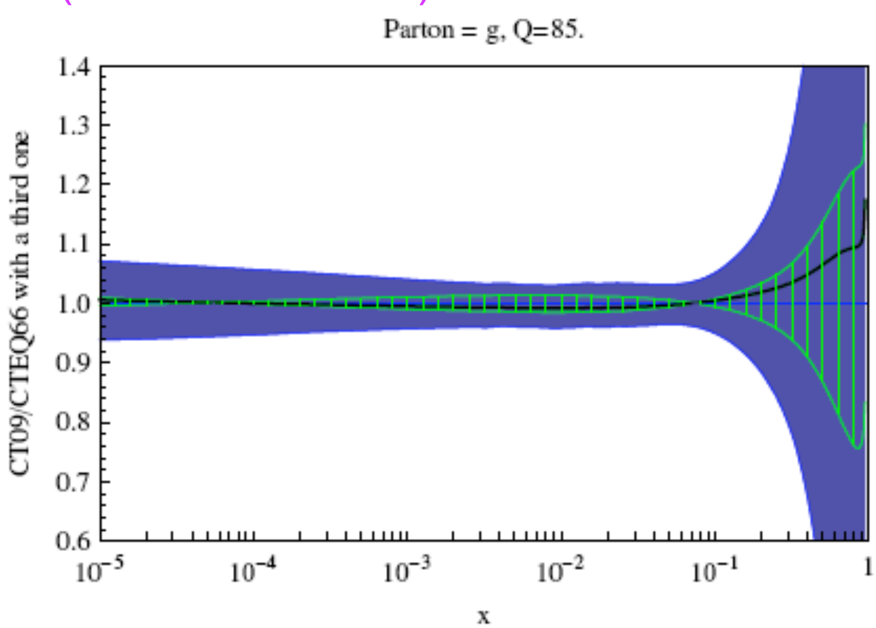

This also means that one can naively scale between 68% and 90% CL.

New from CTEQ-TEA (Tung et al)->CT10 PDFs

- Combined HERA-1 data
- CDF and D0 Run-2 inclusive jet data
- Tevatron Run 2 Z rapidity from CDF and D0
- W electron asymmetry from CDFII and D0II (D0 muon asymmetry) (in CT10W)
- Other data sets same as CTEQ6.6
- All data weights set to unity (except for CT10W)
- Tension observed between D0 II electron asymmetry data and NMC/BCDMS data
- Tension between D0 II electron and muon asymmetry data
- Experimental normalizations are treated on same footing as other correlated systematic errors
- More flexible parametrizations: 26 free parameters (26 eigenvector directions)
- Dynamic tolerance: look for 90% CL along each eigenvector direction
  - within the limits of the quadratic approximation, can scale between 68% and 90% CL with naïve scaling factor
- Two series of PDF's are introduced
  - CT10: no Run 2 W asymmetry
  - CT10W: Run 2 W asymmetry with an extra weight

CT10/CT10W predictions

No big changes with respect to CTEQ6.6

Total cross sections

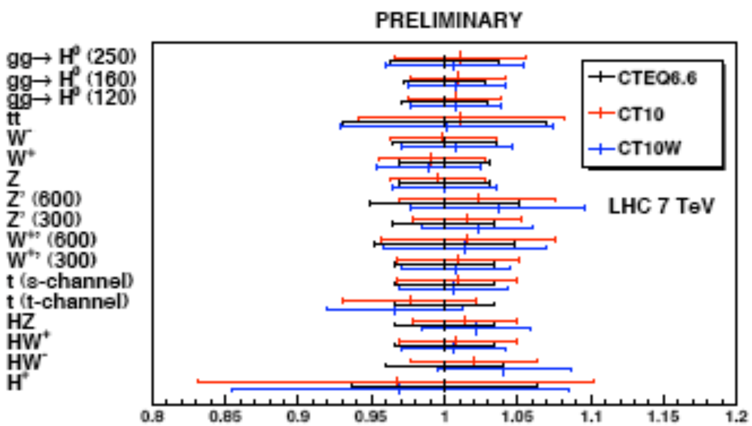

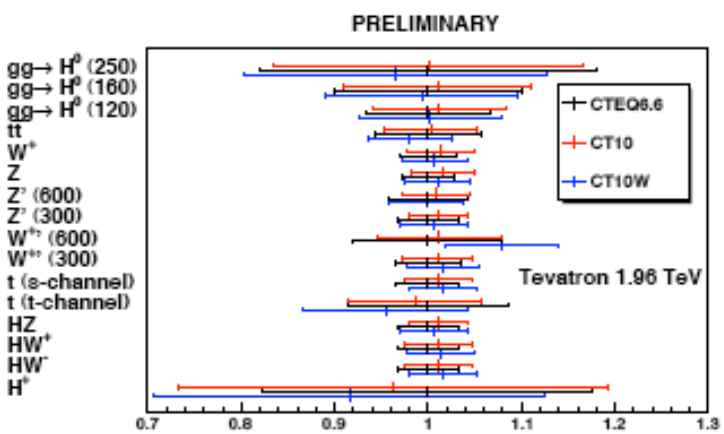

$\sigma(W^+)/\sigma(W^-)$ vs. y_W at the LHC

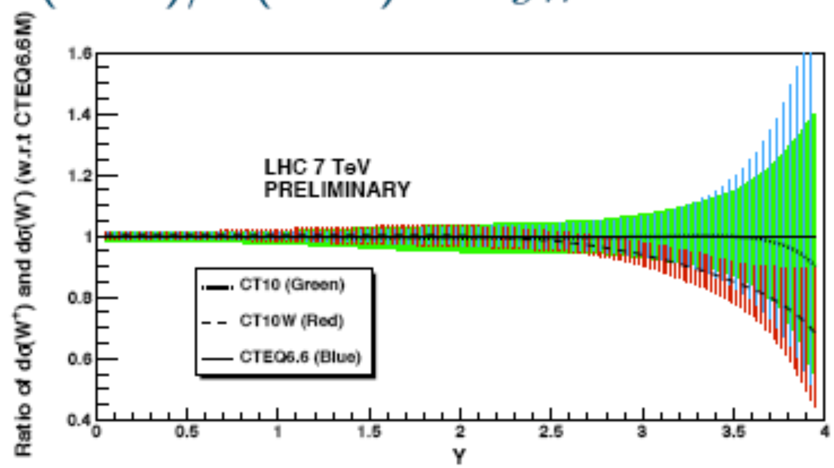

$\sigma(W^\pm)/\sigma(Z^0)$ vs. $y_{W/Z}$ at the LHC

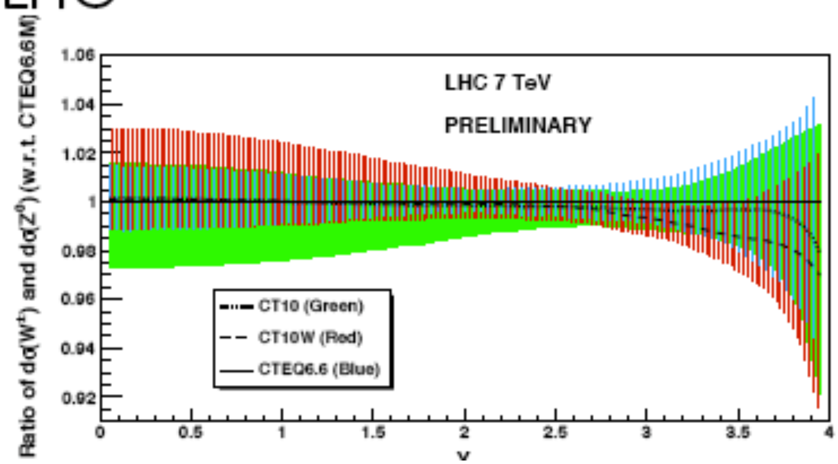

LO PDFs

- Workhorse for many predictions at the LHC are still LO PDFs
- Many LO predictions at the LHC differ significantly from NLO predictions, not because of the matrix elements but because of the PDFs
- W^+ rapidity distribution is the poster child
  - the forward-backward peaking obtained at LO is an artifact
  - large x u quark distribution is higher at LO than NLO due to deficiencies in the LO matrix elements for DIS

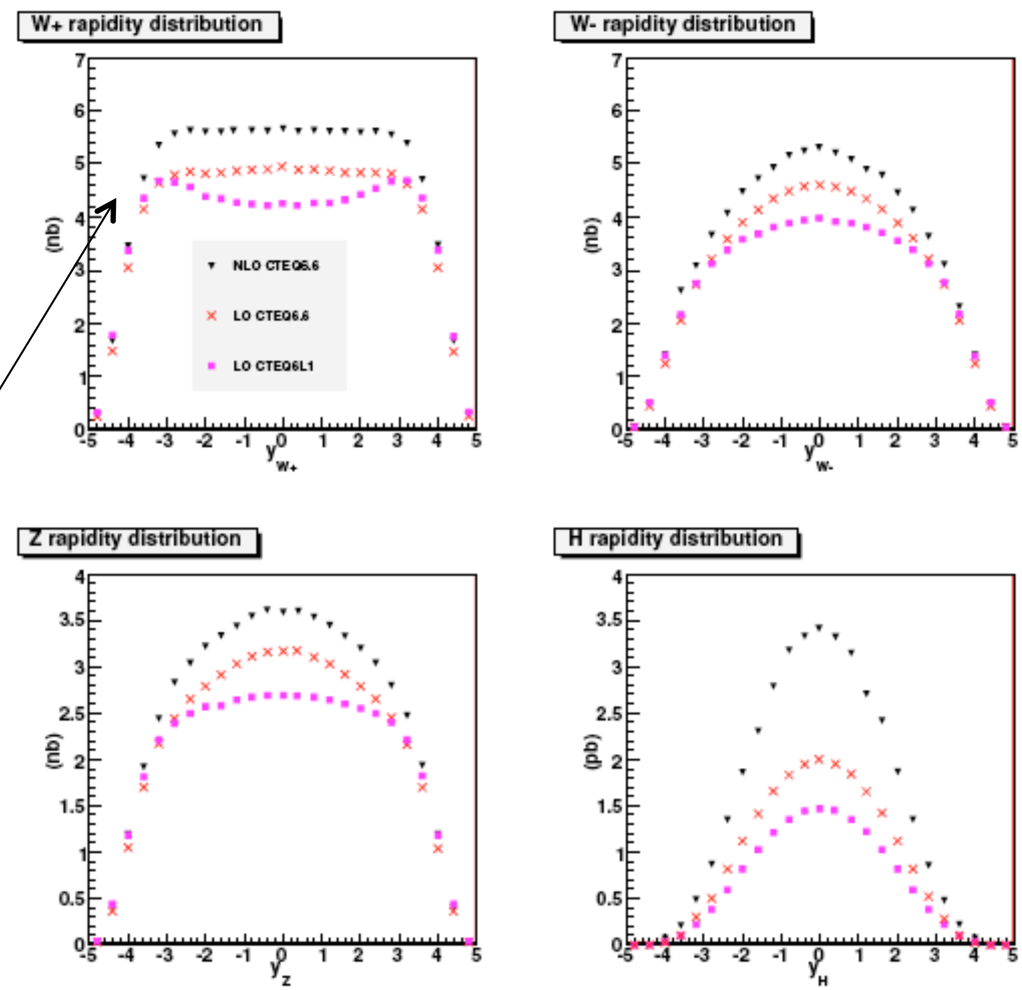

Figure 1. A comparison of the NLO pseudodata for SM boson rapidity distributions (in Δy=0.4 bins) predicted at the LHC (14 TeV) to the respective LO predictions based on CTEQ6.6M and CTEQ6L1 PDFs.

Where are the differences between LO and NLO partons?

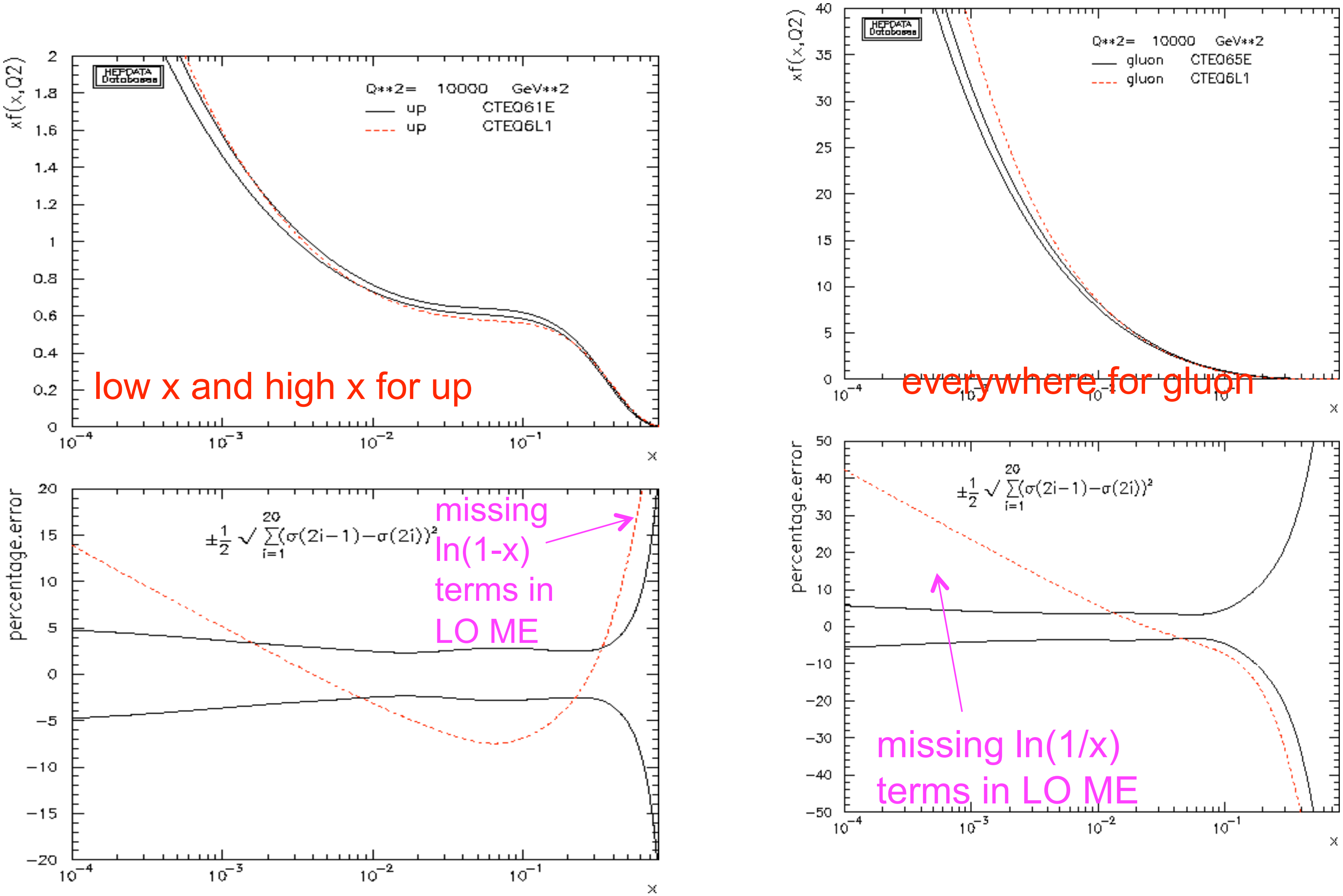

Talking points

- LO* pdf's should behave as LO as x->0; as close to NLO as possible as x->1
- LO* pdf's should describe underlying event at Tevatron with a tune similar to CTEQ6L (for convenience) and extrapolate to a *reasonable* UE at the LHC

Modified LO PDFs

- Try to make up for the deficiencies of LO PDFs by
  - relaxing the momentum sum rule
  - including NLO pseudo-data in the LO fit to guide the modified LO distributions
- Results tend to be in better agreement with NLO predictions, both in magnitude and in shape
- Some might say that the PDFs then have no predictive power, but this is true for any LO PDFs

- See arXiv:0910.4183; PDFs available from LHAPDF
- See arXiv:0711.2473 for MRST2007lomod PDFs

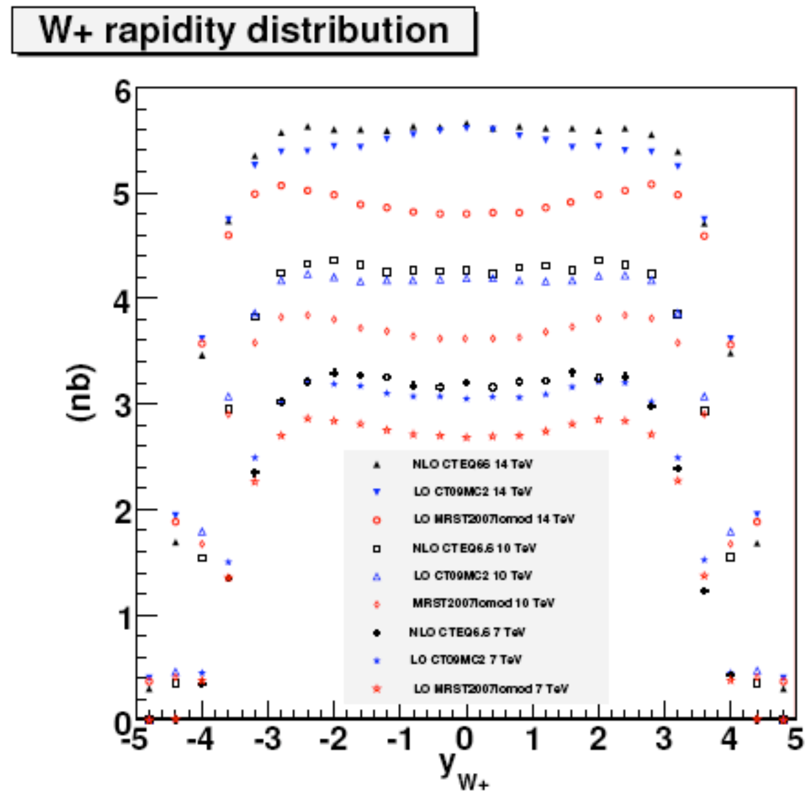

Figure 6. Predictions for the W^+ rapidity distribution at the LHC ($\sqrt{s}$ =7, 10 and 14 TeV) in Δy =0.4 bins, given at NLO using the CTEQ6.6M PDFs, and at LO using the CT09MC2 and MRST2007lomod PDFs. The actual cross sections (without normalization rescaling factors) are shown.

gg->Higgs

- Higgs K-factor is too large to absorb into PDFs (nor would you want to)
- Shape is ok with LO PDF's, improves a bit with the modified LO PDFs

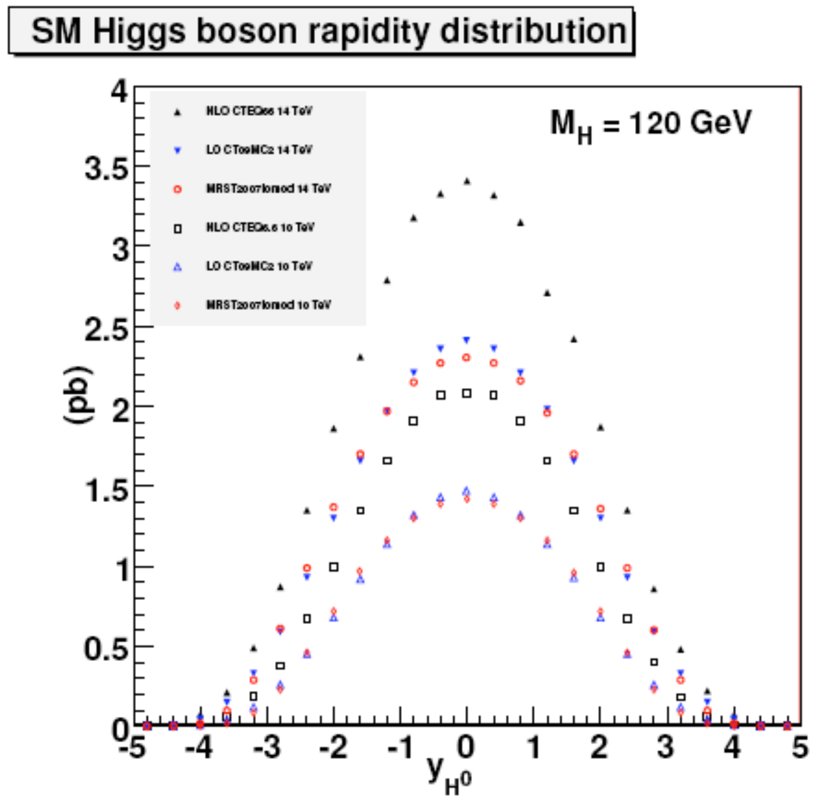

Figure 9. Same as figure 6, for the Higgs boson rapidity distribution at $\sqrt{s}$ =10 and 14 TeV. To maintain legibility, the distribution for $\sqrt{s}$ =7 TeV is not shown.

Tevatron data

- Wealth of data from the Tevatron, both Run 1 and Run 2, that allows us to test/add to our pQCD formalism
- Consider for example W/ Z production
  - cross section increases with center-of-mass energy as expected
- We've already seen that the data is in reasonable agreement with the theoretical predictions

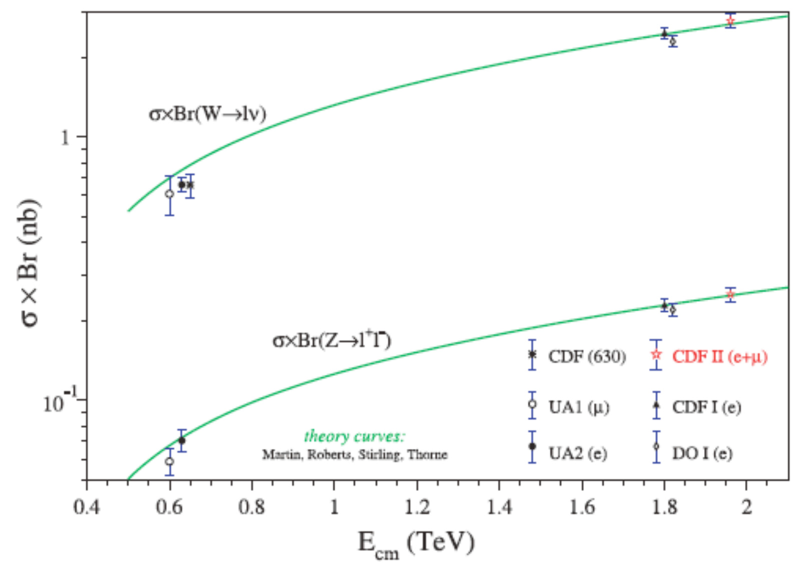

Figure 37. *W* and *Z* cross sections as a function of the centre-of-mass energy.

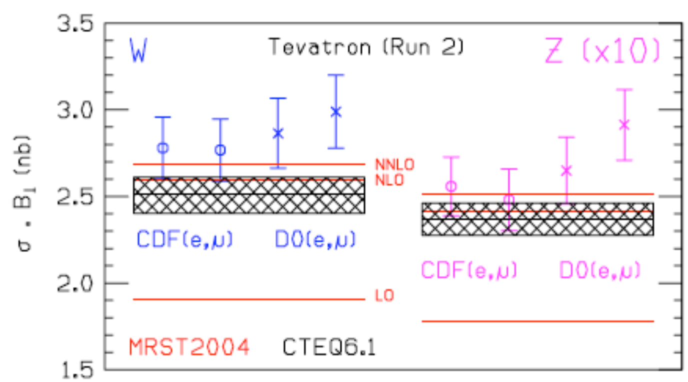

Figure 4. Predictions for the *W* and *Z* total cross sections at the Tevatron and LHC, using MRST2004 [10] and CTEQ6.1 pdfs [11], compared with recent data from CDF and D0. The MRST predictions are shown at LO, NLO and NNLO. The CTEQ6.1 NLO predictions and the accompanying pdf error bands are also shown.

Rapidity distributions

- Effect of NNLO is basically a small normalization shift from NLO
- Data is in good agreement
- Provides some further constraints in pdf fits

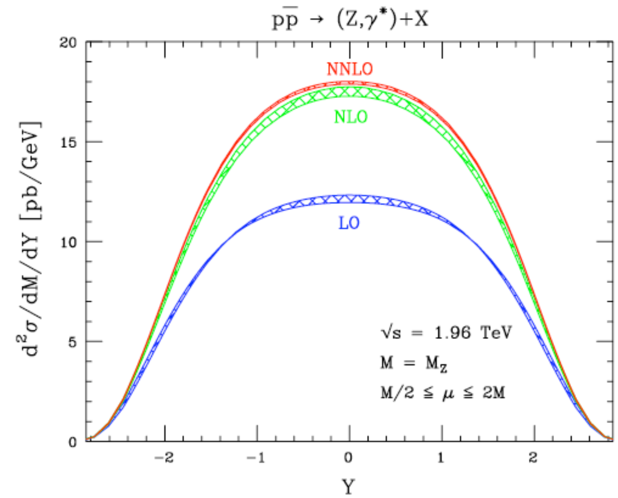

Figure 38. Predictions for the rapidity distribution of an on-shell Z boson in Run 2 at the Tevatron at LO, NLO and NNLO. The bands indicate the variation of the renormalization and factorization scales within the range $M_Z/2$ to $2M_Z$.

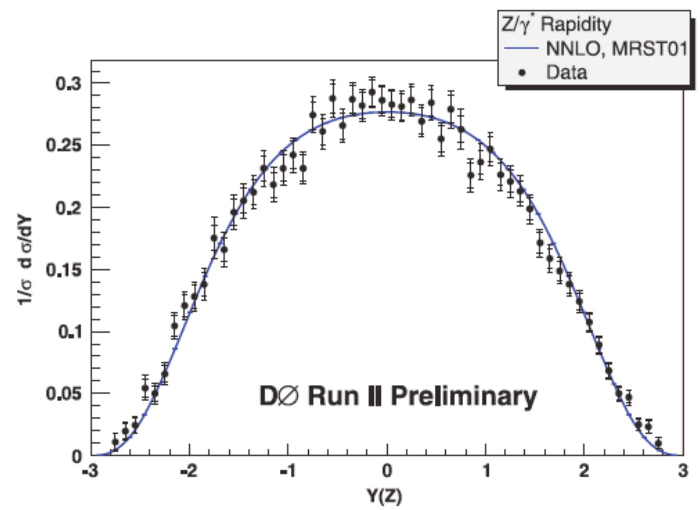

Figure 39. Z rapidity distribution from D0 in Run 2.

Transverse momentum distributions

- Soft (and hard) gluon effects cause W/Z bosons to be produced at non-zero transverse momentum, as we saw last lecture
- Well-described by ResBos and parton shower Monte Carlos
  - although latter need to have non-perturbative k_T added in by hand

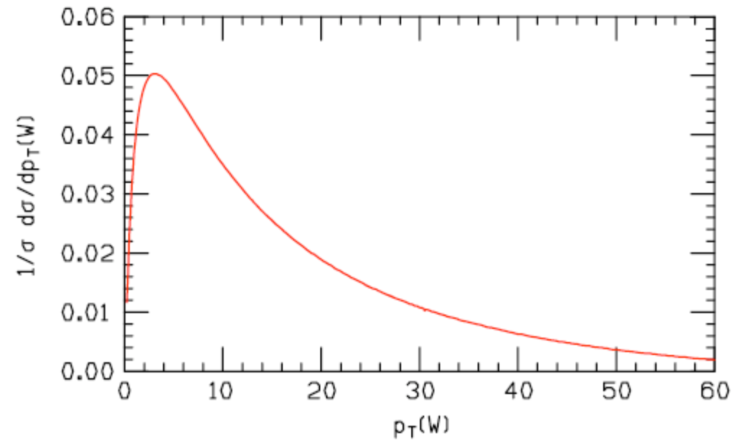

Figure 20. The resummed (leading log) W boson transverse momentum distribution.

CDF Preliminary

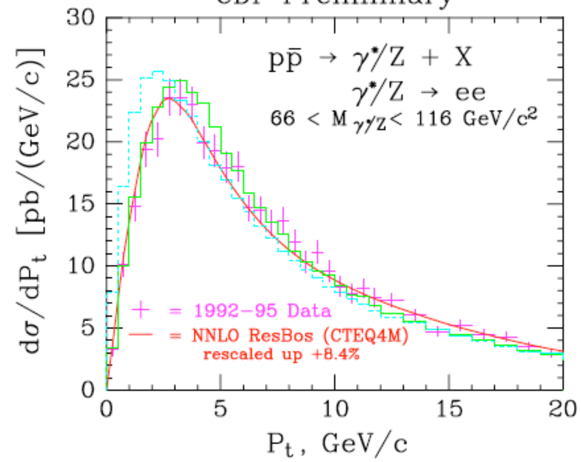

Figure 40. The transverse momentum distribution (low p_T) for $Z \to e^+e^-$ from CDF in Run 1, along with comparisons to predictions from PYTHIA and ResBos. The dashed blue curve is the default PYTHIA prediction. The PYTHIA solid-green curve has had an additional 2 GeV of k_T added to the parton shower.

p_T distributions

- High p_T region is due to hard gluon(s) emission, but is also well-described by predictions such as ResBos
- If we look at average transverse momentum of Drell-Yan pairs as a function of mass, we see that there is an increase that is roughly logarithmic with the mass
  - as expected from the logs that we saw accompanying soft gluon emission

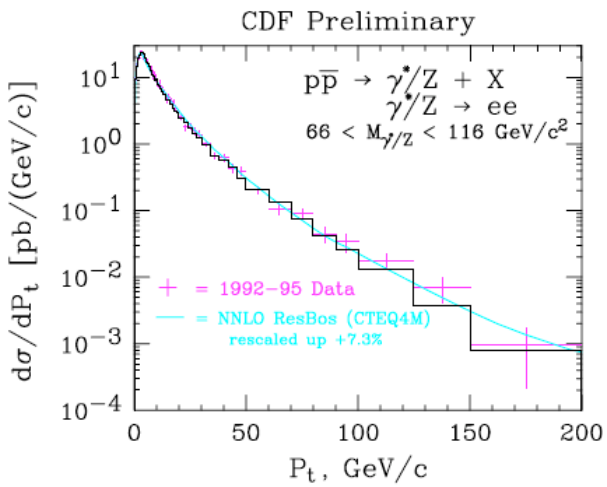

Figure 41. The transverse momentum distribution (full p_T range) for $Z \to e^+e^-$ from CDF in Run 1, along with comparisons to predictions from PYTHIA (solid histogram) and ResBos.

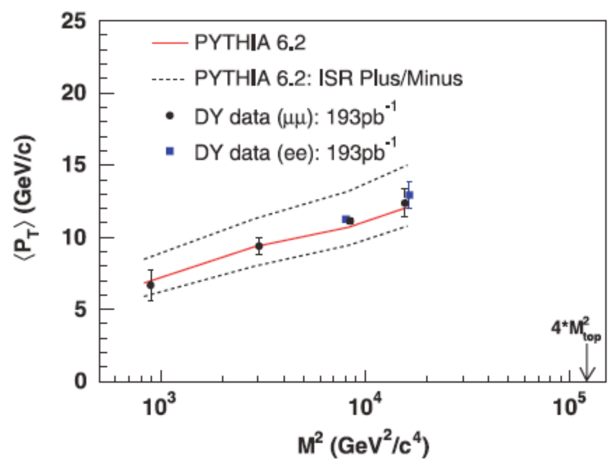

Figure 42. The average transverse momentum for Drell–Yan pairs from CDF in Run 2, along with comparisons to predictions from PYTHIA.

Inclusive jet production

- This cross section/ measurement spans a very wide kinematical range, including the highest transverse momenta (smallest distance scales) of any process
- Note in the cartoon to the right that in addition to the 2->2 hard scatter that we are interested in, we also have to deal with the collision of the remaining constituents of the proton and anti-proton (the "underlying event")
- This has to be accounted for/ subtracted for any comparisons of data to pQCD predictions

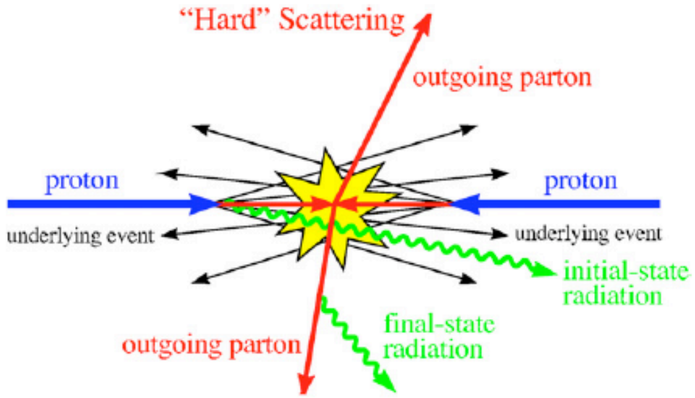

Figure 43. Schematic cartoon of a 2 → 2 hard-scattering event.

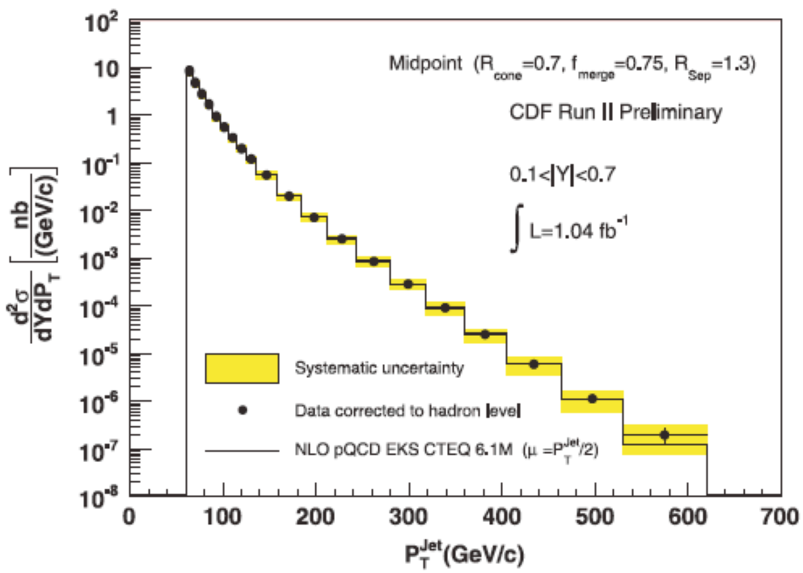

Figure 44. The inclusive jet cross section from CDF in Run 2.

Study of inclusive jet events

- Look at the charged particle transverse momenta in the regions transverse to the dijet direction
- Label the one with the larger amount of transverse momenta the max direction and the one with the smaller amount the min direction
- The momenta in the max direction increases with the p_T of the lead jet, while the momenta in the min cone is constant and is approximately equal to that in a minimum bias event
- "Tunes" to the underlying event model in parton shower Monte Carlos can correctly describe both the max and min regions and can be used for the correct subtraction of UE energy in jet measurements

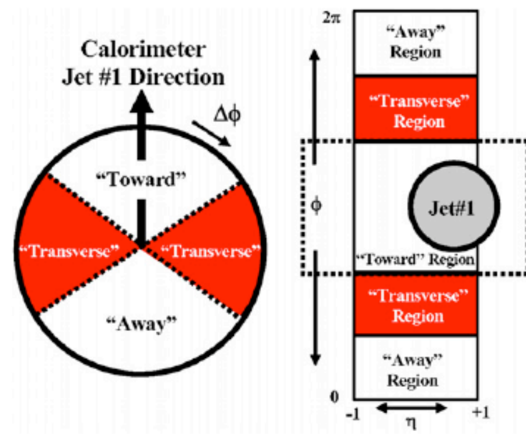

Figure 45. Definition of the 'toward', 'away' and 'transverse' regions.

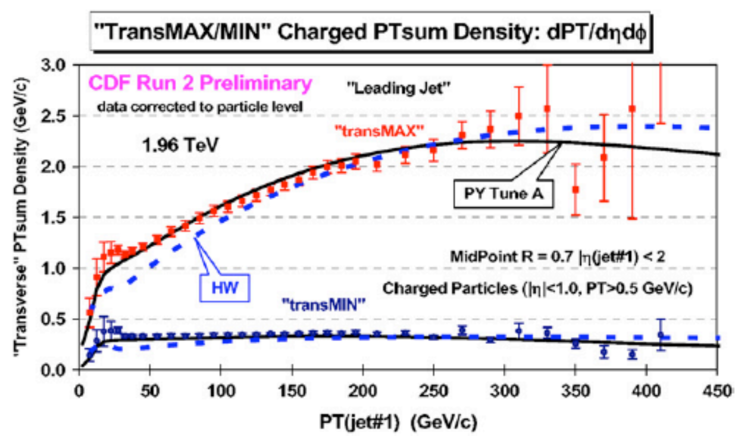

Figure 46. The sum of the transverse momenta of charged particles inside the TransMAX and TransMIN regions, as a function of the transverse momentum of the leading jet.

Hadronization

- Parton showers in the initial and final state produce a large multiplicity of gluons
- The parton shower evolution variable *t* decreases (for the final state) from a scale similar to the scale of the hard scatter to a scale at which pQCD is no longer applicable (near Λ_{QCD})
- At this point, we must construct models as to how the colored quarks and gluons recombine to form the (colorless) final state hadrons
- The two most popular models are the cluster and string models

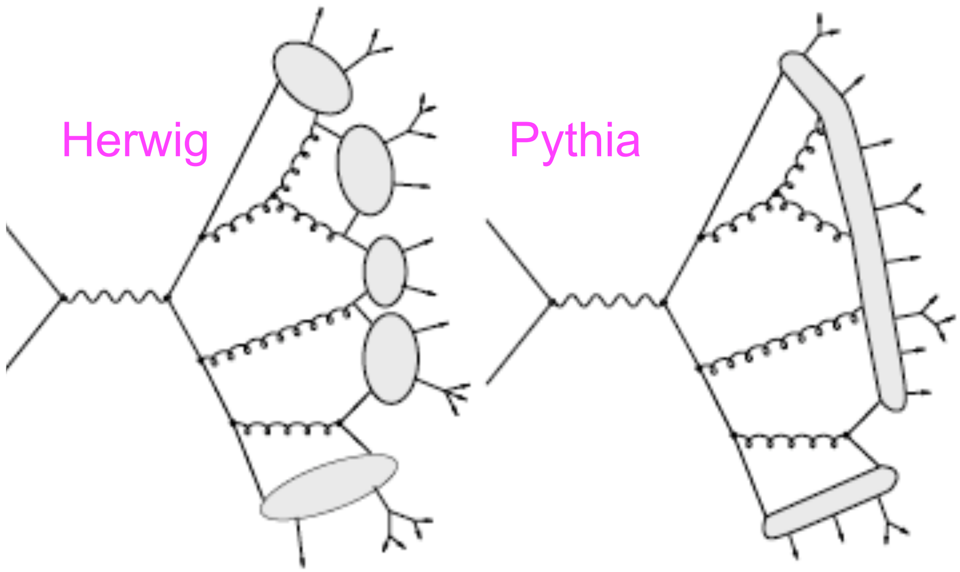

Figure 2: Cluster and string hadronization models.

•In cluster model, there is a non-perturbative splitting of gluons into q-qbar pairs; color-singlet combinations of q-qbar pairs form clusters which isotropically decay into pairs of hadrons
•In string model, relativistic string represents color flux; string breaks up into hadrons via q-qbar production in its intense color field

Corrections

- Hadron to parton level corrections
  - subtract energy from the jet cone due to the underlying event
  - add energy back due to hadronization
    - partons whose trajectories lie inside the jet cone produce hadrons landing outside

…partially cancel, but UE correction is larger for cone of 0.7
hadronization corrections for Pythia and Herwig basically identical

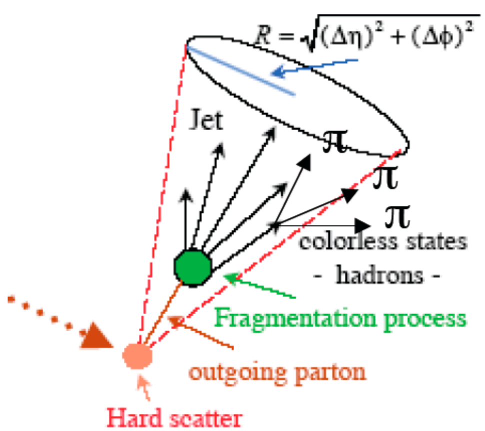

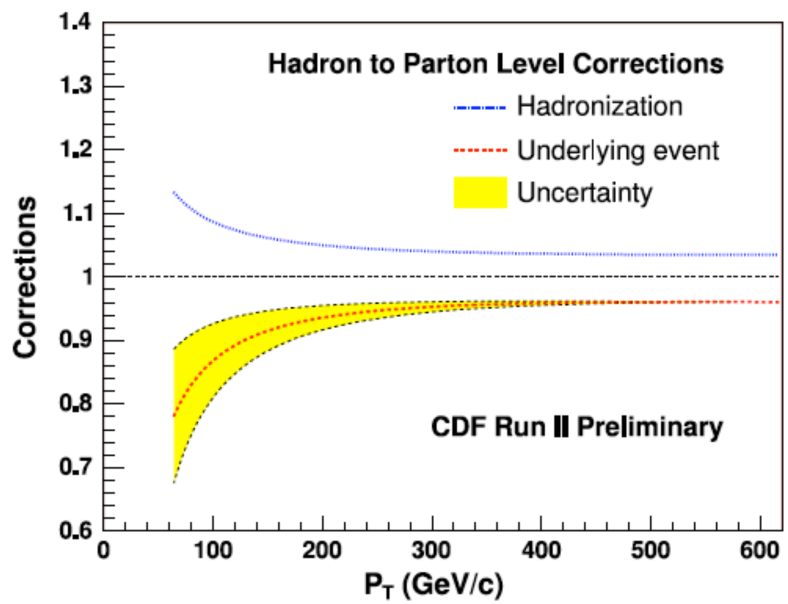

Figure 48. Fragmentation and underlying event corrections for the CDF inclusive jet result, for a cone size $R = 0.7$.

Hadronization corrections

- Can do a back-of –the-envelope calculation with a Field-Feynman-like model

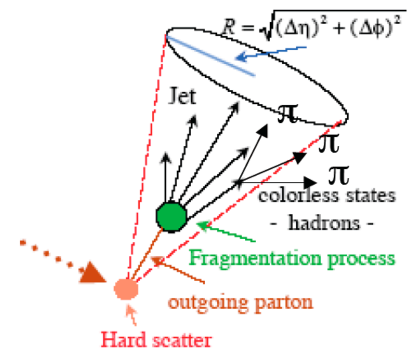

Splash-out. Some of the partonic transverse energy can leak out of the jet cone. The order α_s^3 perturbation theory gets this effect partly right: in a three parton final state the third parton can escape the jet cone. However, using the picture embedded in Monte Carlo models, the late stages of partonic branching and the final hadronization of the partons can also result in transverse energy escaping the jet cone. Here is a simple model for this effect.

Consider the hadrons that represent the decay products of a high E_T parton. Let η be the rapidity of the hadrons relative to jet axis. Let $\vec{k}_T$ be the transverse momentum of the particles relative to jet axis. Let the distribution of hadrons be

$$\frac{dN}{d\eta d\vec{k}_T} = \frac{A}{\pi \langle k_T^2 \rangle} \exp\left\{-k_T^2 / \langle k_T^2 \rangle\right\}, \tag{10}$$

where A is the number of hadrons per unit rapidity and $\langle k_T^2 \rangle$ is average k_T^2 of the hadrons. Then the E_T lost is approximately

$$E_T^{\rm out} = \int_0^{\eta_1} d\eta \int d\vec{k}_T \, \frac{1}{2} |\vec{k}_T| e^{\eta} \, \frac{dN}{d\eta d\vec{k}_T}, \tag{11}$$

where $\eta_1 = -\ln\left(\tan(R/2)\right)$. Performing the integral gives

$$E_T^{\rm out} = \frac{\sqrt{\pi}}{4} A \sqrt{\langle k_T^2 \rangle} \left(e^{\eta_1} - 1\right). \tag{12}$$

Taking $\sqrt{\langle k_T^2 \rangle} = 0.3$ GeV and[10] $A = 5$, I find

$$E_T^{\rm out} \approx 1.1 \text{ GeV}. \tag{13}$$

Hadronization corrections

- Or can study a parton shower Monte Carlo with hadronization on/off
  - and again find on the order of 1 GeV/c (for a cone of radius 0.7 at the Tevatron)
  - NB: hadronization correction for NLO (at most 2 partons in a jet) = the correction for parton showers (many partons in a jet) to the extent that the jet shapes are the same at the NLO and parton shower level
- What is the dependence of the hadronization corrections (also called splashout) on jet transverse momentum?
  - not so much (as Borat might say)
- This may seem surprising (that the correction does not increase with the jet p_T)
- But jets get narrower as the p_T increases (see later), so the parton level energy in the outermost annulus of the jet (where the splashout originates) is fairly constant as a function of jet p_T

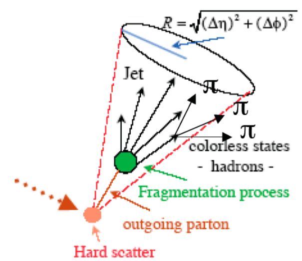

Corrections

- Hadron to parton level corrections
  - subtract energy from the jet cone due to the underlying event
  - add energy back due to hadronization
    - partons whose trajectories lie inside the jet cone produce hadrons landing outside
- Corrections determined by Monte Carlo, turning on/off each element
  - possible because the UE was tuned to describe global event characteristics at the Tevatron
- Result is in good agreement with NLO pQCD predictions using CTEQ6.1 pdf's
  - pdf uncertainty is similar to experimental systematic errors

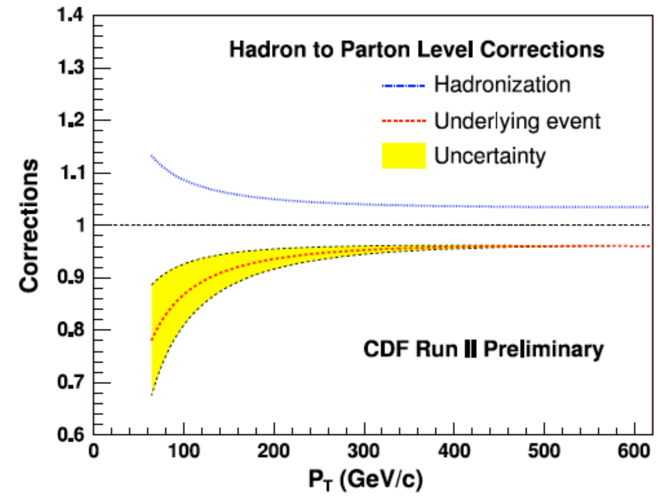

Figure 48. Fragmentation and underlying event corrections for the CDF inclusive jet result, for a cone size $R = 0.7$.

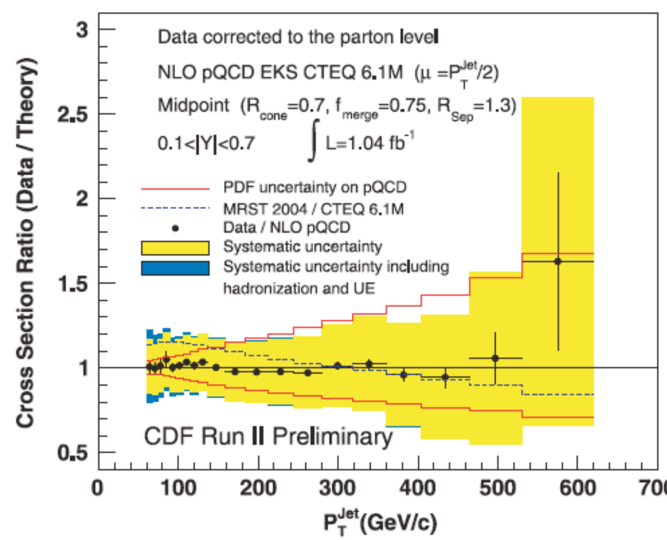

Figure 49. The inclusive jet cross section from CDF in Run 2 compared on a linear scale to NLO theoretical predictions using CTEQ6.1 and MRST2004 pdfs.

Inclusive jet cross section

new physics tends to be central

pdf explanations are universal

crucial to measure over a wide rapidity interval

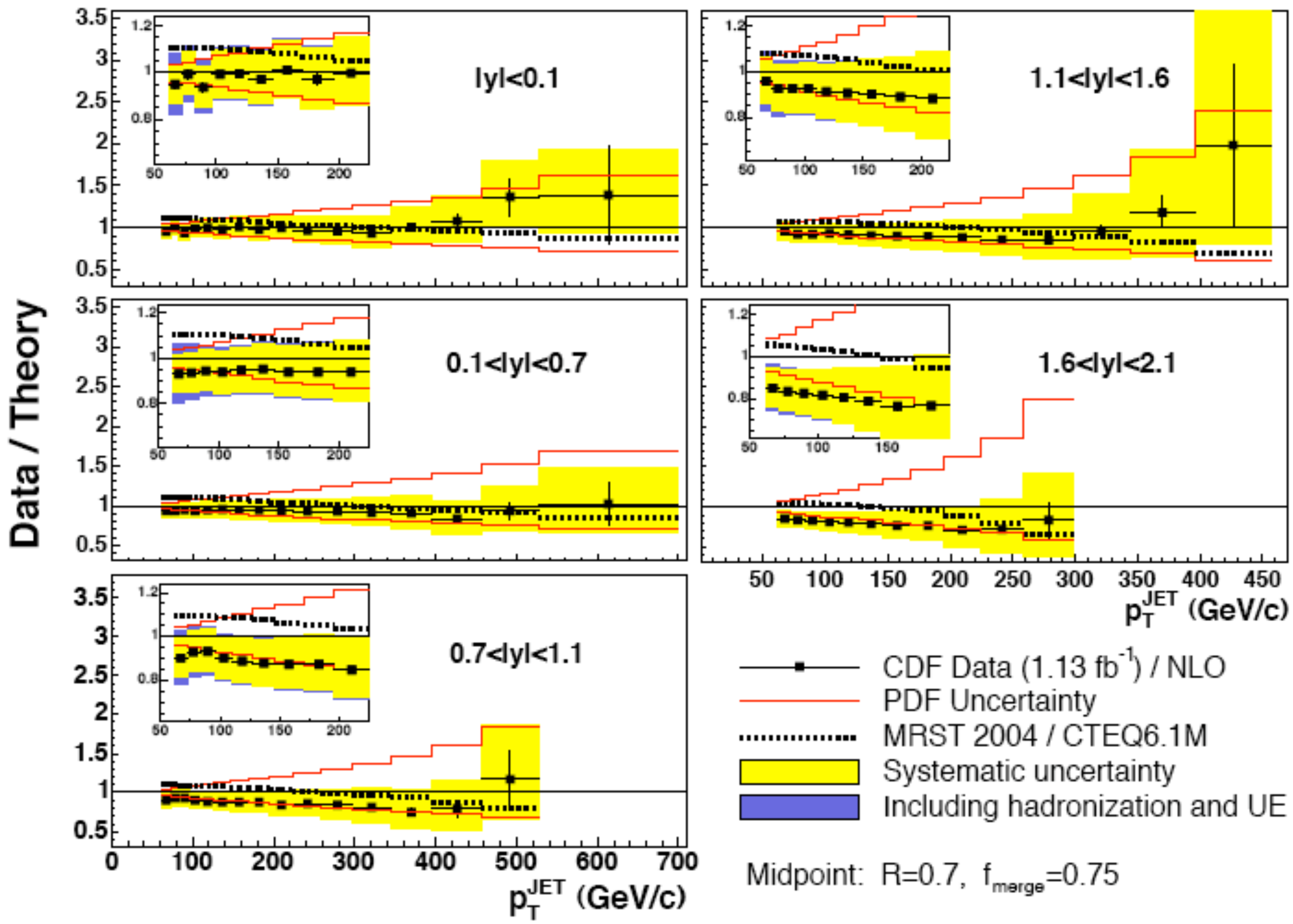

Full disclosure for experimentalists

- Every cross section should be quoted at the hadron level with an explicit correction given between the hadron and parton levels

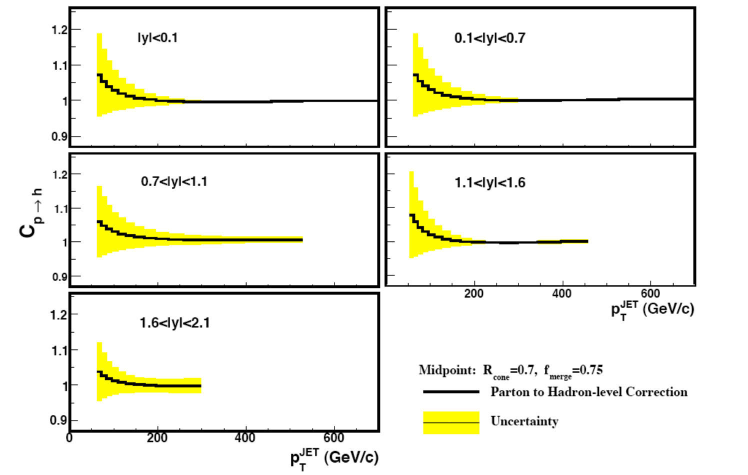

TABLE IX: Measured inclusive jet cross sections as a function of p_T for jets in the region $0.1 < |y| < 0.7$ together with the statistical (*stat.*) and systematic (*sys.*) uncertainties. The bin-by-bin parton-to-hadron-level ($C_{p\rightarrow h}$) corrections are also shown.

regions. The correction is derived from PYTHIA (solid line) for the correction is conservatively taken as the systematic

	$0.1 < \lvert y\rvert < 0.7$	
p_T (GeV/c)	$\sigma \pm (stat.) \pm (sys.)$ [nb/(GeV/c)]	$C_{p\rightarrow h}$
62 – 72	$(6.28 \pm 0.04^{+0.59}_{-0.56}) \times 10^{0}$	1.072 ± 0.108
72 – 83	$(2.70 \pm 0.02^{+0.26}_{-0.25}) \times 10^{0}$	1.055 ± 0.088
83 – 96	$(1.15 \pm 0.01^{+0.11}_{-0.11}) \times 10^{0}$	1.041 ± 0.071
96 – 110	$(4.88 \pm 0.03^{+0.51}_{-0.48}) \times 10^{-1}$	1.030 ± 0.057
110 – 127	$(2.07 \pm 0.01^{+0.22}_{-0.21}) \times 10^{-1}$	1.022 ± 0.045
127 – 146	$(8.50 \pm 0.04^{+0.98}_{-0.91}) \times 10^{-2}$	1.015 ± 0.035
146 – 169	$(3.30 \pm 0.01^{+0.41}_{-0.38}) \times 10^{-2}$	1.010 ± 0.027
169 – 195	$(1.24 \pm 0.01^{+0.17}_{-0.15}) \times 10^{-2}$	1.006 ± 0.020
195 – 224	$(4.55 \pm 0.05^{+0.67}_{-0.61}) \times 10^{-3}$	1.003 ± 0.014
224 – 259	$(1.56 \pm 0.01^{+0.25}_{-0.23}) \times 10^{-3}$	1.002 ± 0.010
259 – 298	$(4.94 \pm 0.06^{+0.91}_{-0.80}) \times 10^{-4}$	1.001 ± 0.006
298 – 344	$(1.42 \pm 0.02^{+0.30}_{-0.26}) \times 10^{-4}$	1.000 ± 0.003
344 – 396	$(3.53 \pm 0.08^{+0.85}_{-0.73}) \times 10^{-5}$	1.001 ± 0.001
396 – 457	$(6.87 \pm 0.35^{+1.93}_{-1.64}) \times 10^{-6}$	1.001 ± 0.000
457 – 527	$(1.22 \pm 0.13^{+0.40}_{-0.34}) \times 10^{-6}$	1.003 ± 0.001
527 – 700	$(7.08 \pm 1.97^{+3.09}_{-2.54}) \times 10^{-8}$	1.005 ± 0.001

note the correction rapidly approaches unity

Jet Shapes

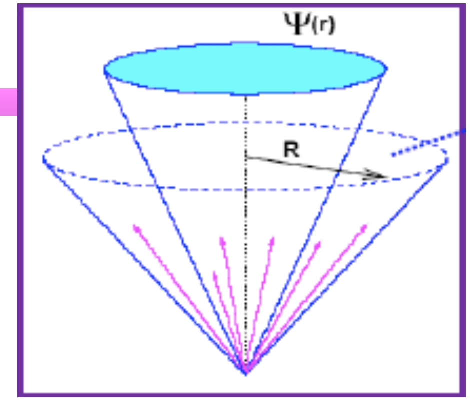

- Jets get narrower as the jet p_T increases
  - smaller rate of hard gluon emission as α_s decreases (can be used to try to determine α_s)
  - jets switch from being gluon-induced to quark-induced

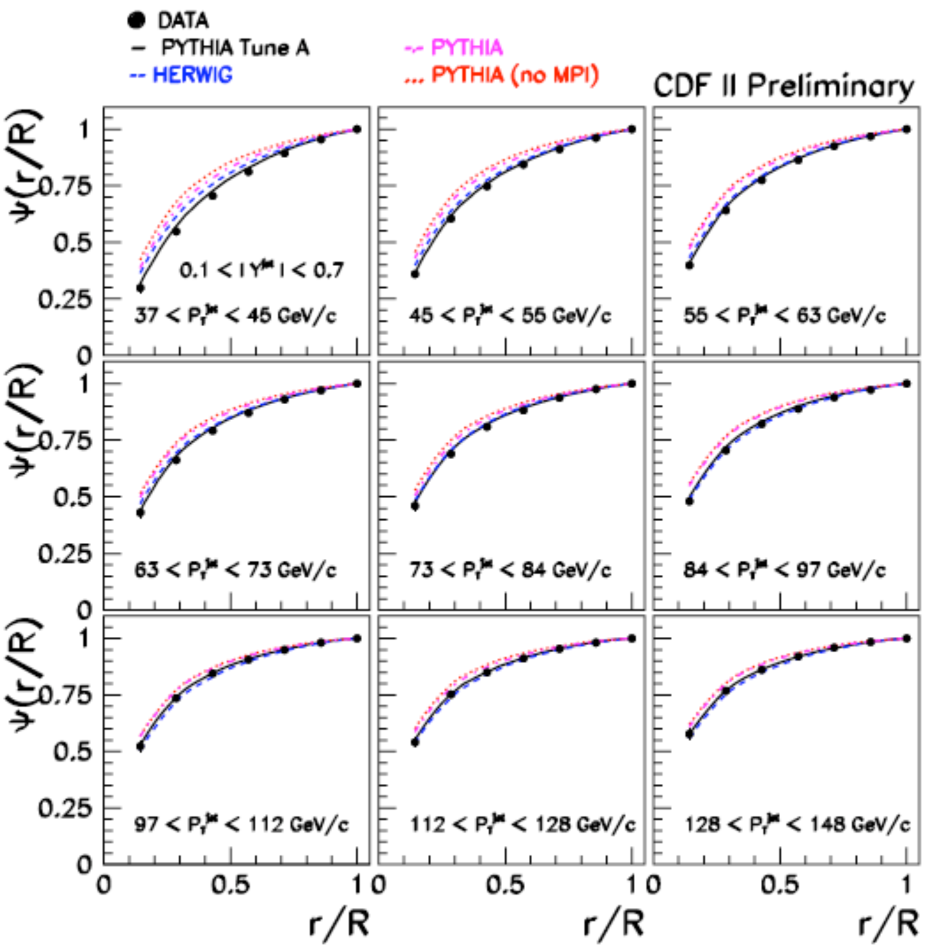

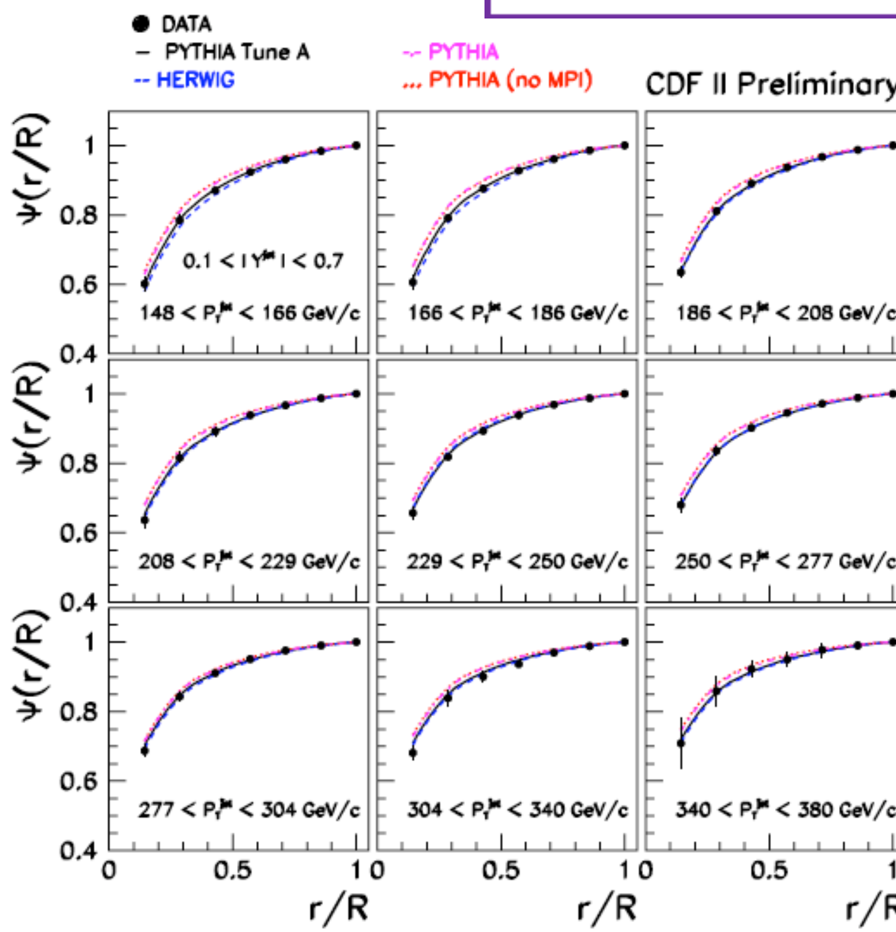

Jet Shapes: quark and gluon differences

- Pythia does a good job of describing jet shapes
  - parton showering + hadronization + multiple parton interactions
- If effects of the underlying event are subtracted out, NLO (where a jet is described by at most two partons) also describes the jet shapes well

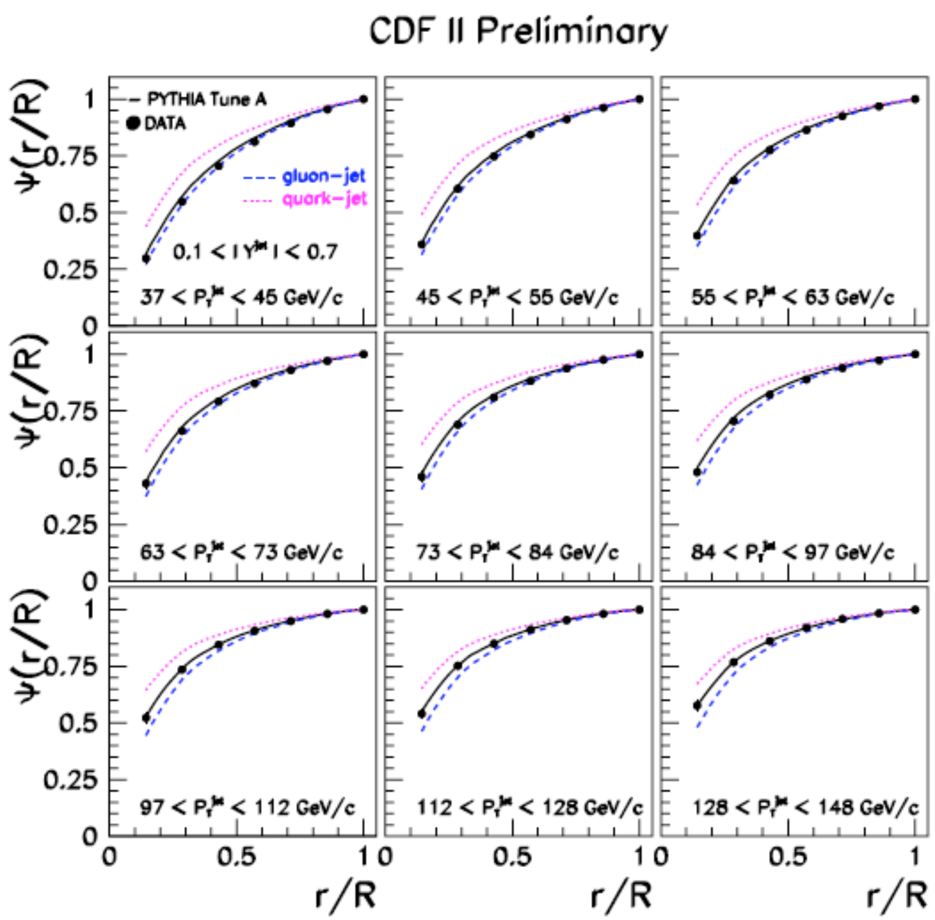

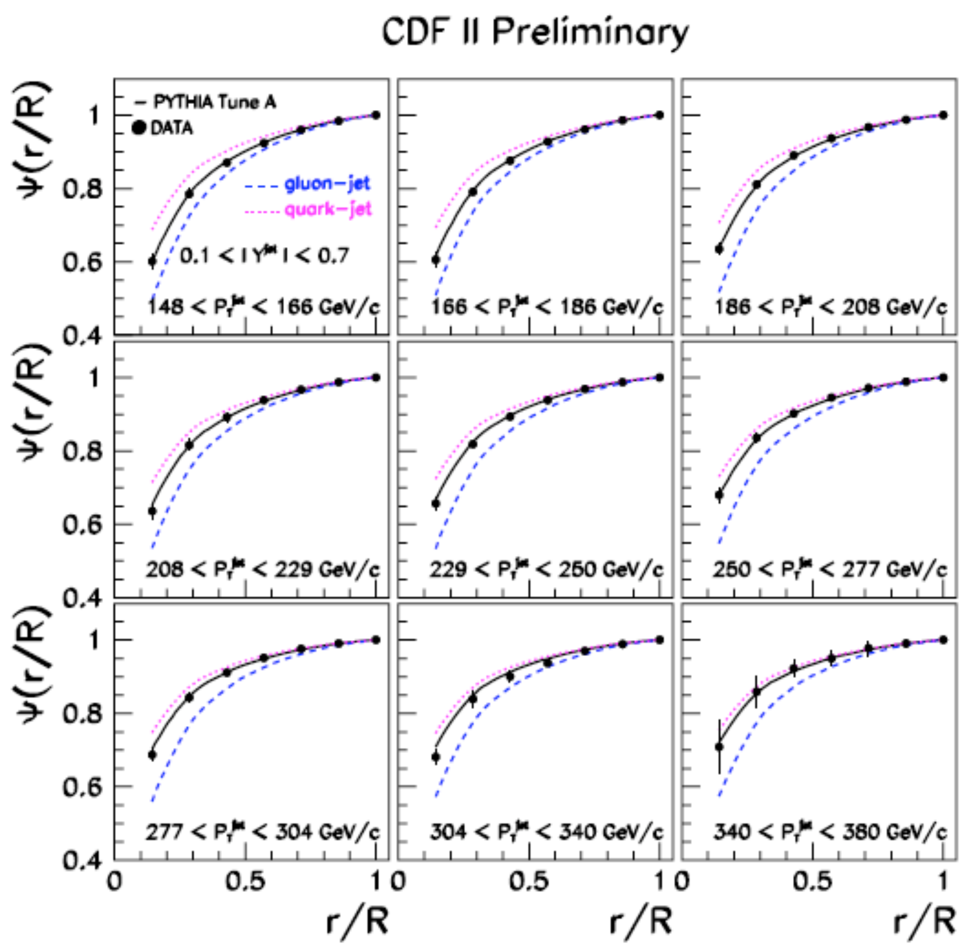

Quark/gluon jet shape differences

- Quarks and gluons radiate proportional to their color factors

$$r \equiv \frac{\langle n_g \rangle}{\langle n_q \rangle} \equiv \frac{\langle \text{gluon jet multiplicity} \rangle}{\langle \text{quark jet multiplicity} \rangle}$$

- At leading order

$$r = \frac{\langle C_A \rangle}{\langle C_F \rangle} = \frac{9}{4} = 2.25$$

- With higher order corrections, r~1.5

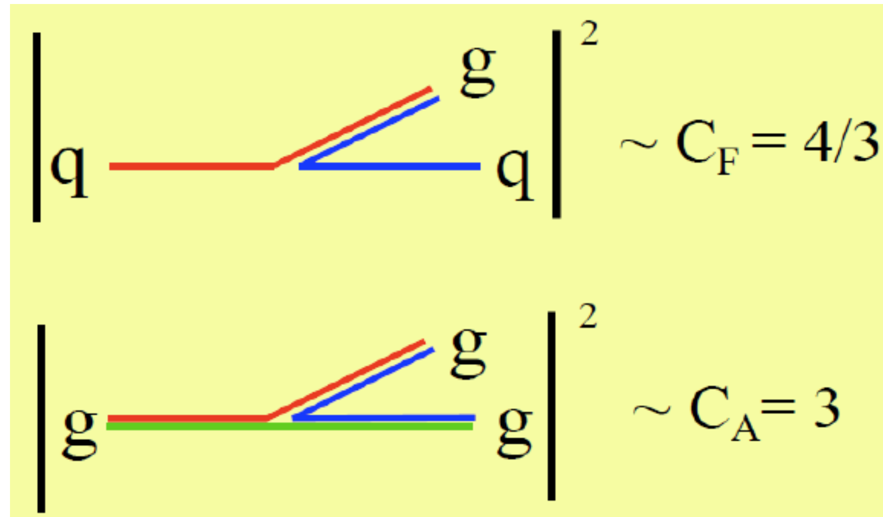

Jet shapes

- Look at the fraction of jet energy in cone of radius 0.7 that is outside the "core" (0.3)
- Gluon jets are always broader than quark jets, but both get narrower with increasing jet p_T
- How to correct for the jet energy outside the prescribed cone?
  - a NLO calculation "knows" about the energy outside the cone, so no correction is needed/wanted
  - for LO comparisons, can correct based on Monte Carlo simulations

at small p_T, jet production dominated by gg and gq scattering due to large gluon distribution at low x

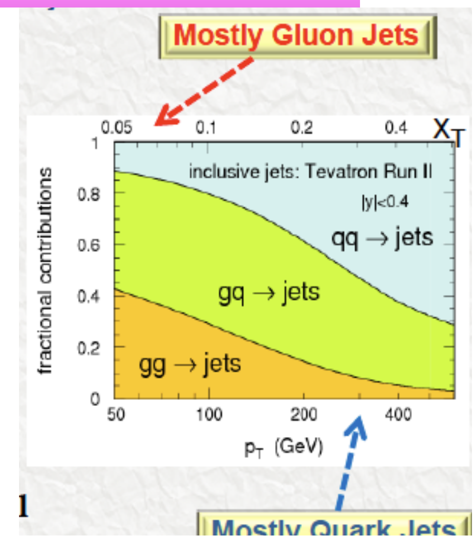

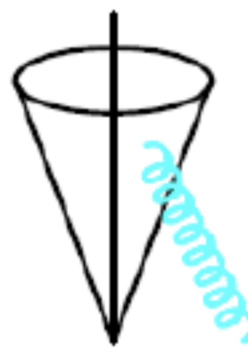

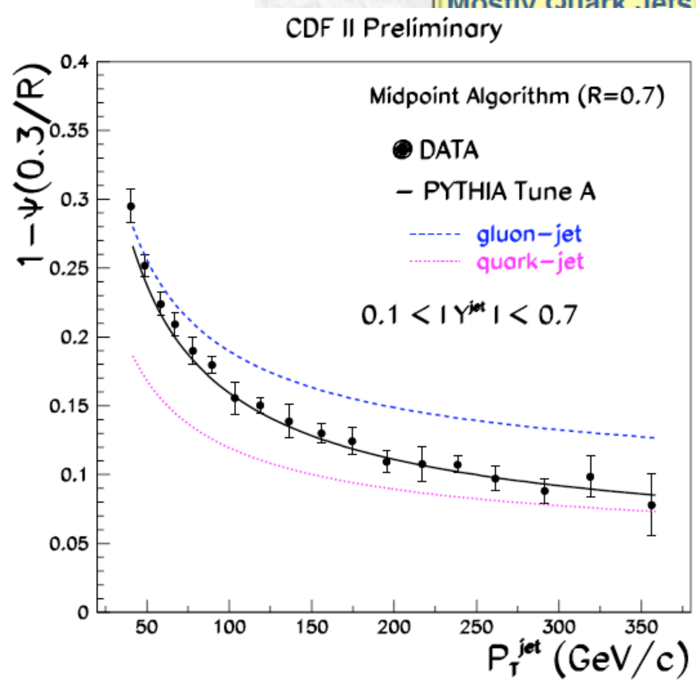

Back to jet algorithms

- For some events, the jet structure is very clear and there's little ambiguity about the assignment of towers to the jet
- But for other events, there is ambiguity and the jet algorithm must make decisions that impact precision measurements
- If comparison is to hadron-level Monte Carlo, then hope is that the Monte Carlo will reproduce all of the physics present in the data and influence of jet algorithms can be understood
  - more difficulty when comparing to parton level calculations

CDF Run II events

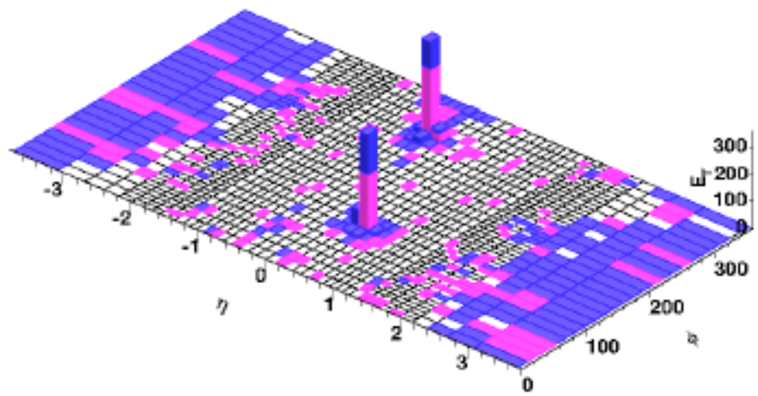

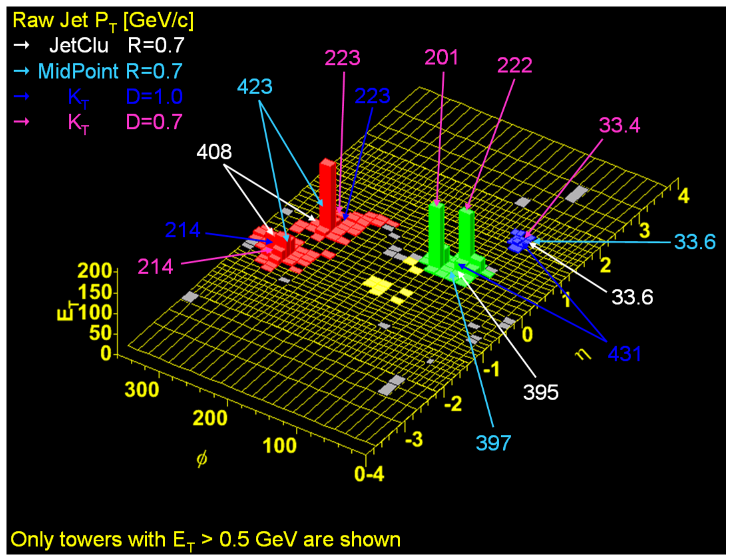

Jets in real life

- Jets don't consist of 1 fermi partons but have a spatial distribution
- Can approximate jet shape as a Gaussian smearing of the spatial distribution of the parton energy
  - the effective sigma ranges between around 0.1 and 0.3 depending on the parton type (quark or gluon) and on the parton p_T
- Note that because of the effects of smearing that
  - the midpoint solution is (**almost always**) lost
    - thus region II is effectively truncated to the area shown on the right
  - the solution corresponding to the lower energy parton can also be lost
    - resulting in dark towers

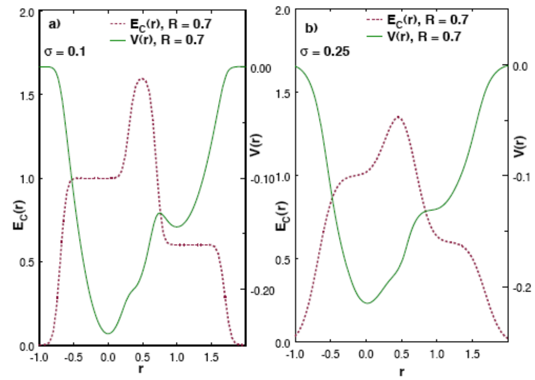

Figure 52. A schematic depiction of the effects of smearing on the midpoint cone jet clustering algorithm

remember the Snowmass potentials

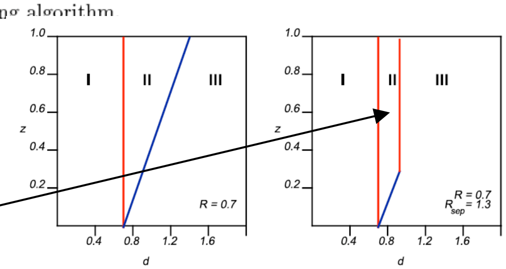

Figure 22. The parameter space (d,Z) for which two partons will be merged into a single jet.

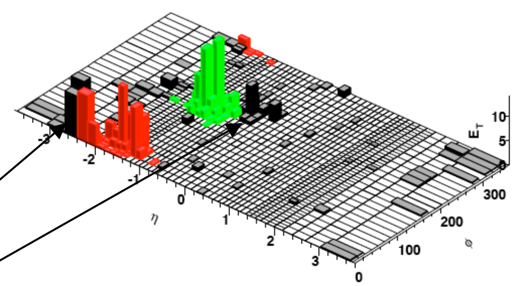

Figure 50. An example of a Monte Carlo inclusive jet event where the midpoint algorithm has left substantial energy unclustered.

Jets in real life

- In NLO theory, can mimic the impact of the truncation of Region II by including a parameter called R_{sep}
  - only merge two partons if they are within R_{sep}*R_{cone} of each other
    - R_{sep}~1.3
  - ~4-5% effect on the theory cross section; effect is smaller with the use of p_T rather than E_T
  - really upsets the theorists (but there are also disadvantages)
- Dark tower effect is also on order of few (<5)% effect on the (experimental) cross section
- Dark towers affect every cone algorithm

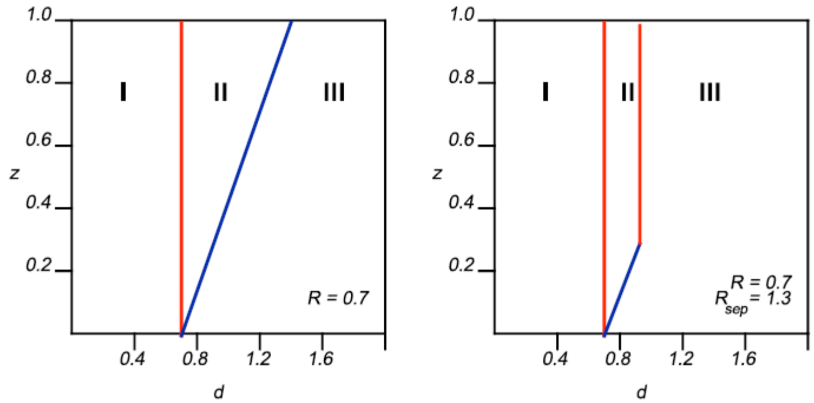

Figure 22. The parameter space (d,Z) for which two partons will be merged into a single jet.

Comparison of k_T and cone results

- Remember
  - at NLO the k_T algorithm corresponds to Region I (for D=R); <u>thus at parton level, the cone algorithm is always larger than the k_T algorithm</u>
- Let's check this out with CDF results after applying hadronization corrections
- Nice confirmation of the perturbative picture

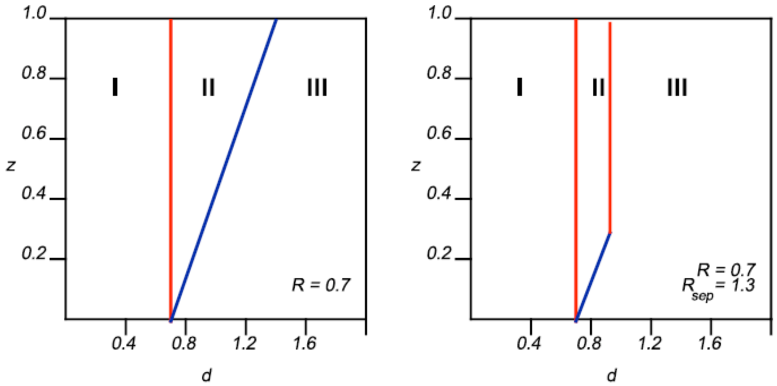

Figure 22. The parameter space (d,Z) for which two partons will be merged into a single jet.

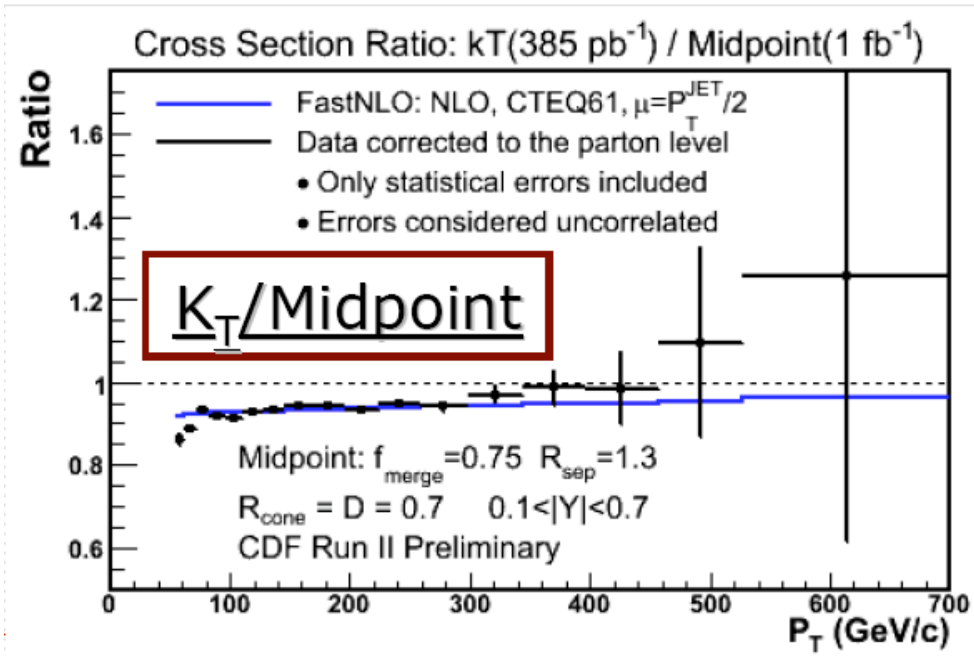

k_T/midpoint ratios for all rapidities

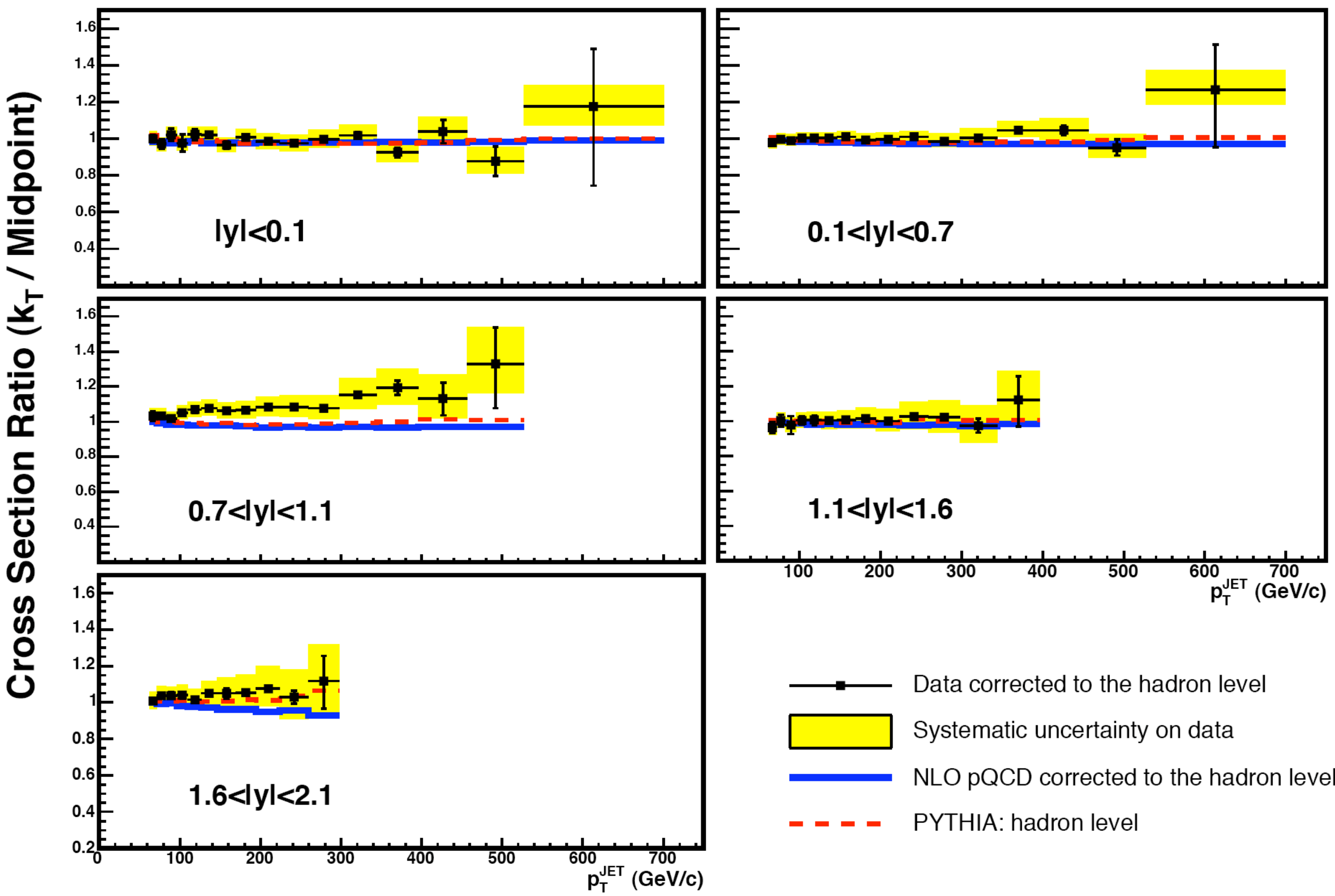

FIG. 17: The ratios of the inclusive jet cross sections measured using the k_T algorithm with $D = 0.7$ [9] to those measured using the Midpoint jet finding algorithm with $R_{\rm cone} = 0.7$ in this paper (points). The systematic uncertainty on the ratio is given as the yellow band. The predictions from NLO pQCD (solid lines) and PYTHIA (dashed lines) for this ratio are also shown.

SISCone vs Midpoint

- The SISCone jet algorithm developed by Salam et al is preferred from a theoretical basis, as there is less IR sensitivity from not requiring any seeds as the starting point of a jet

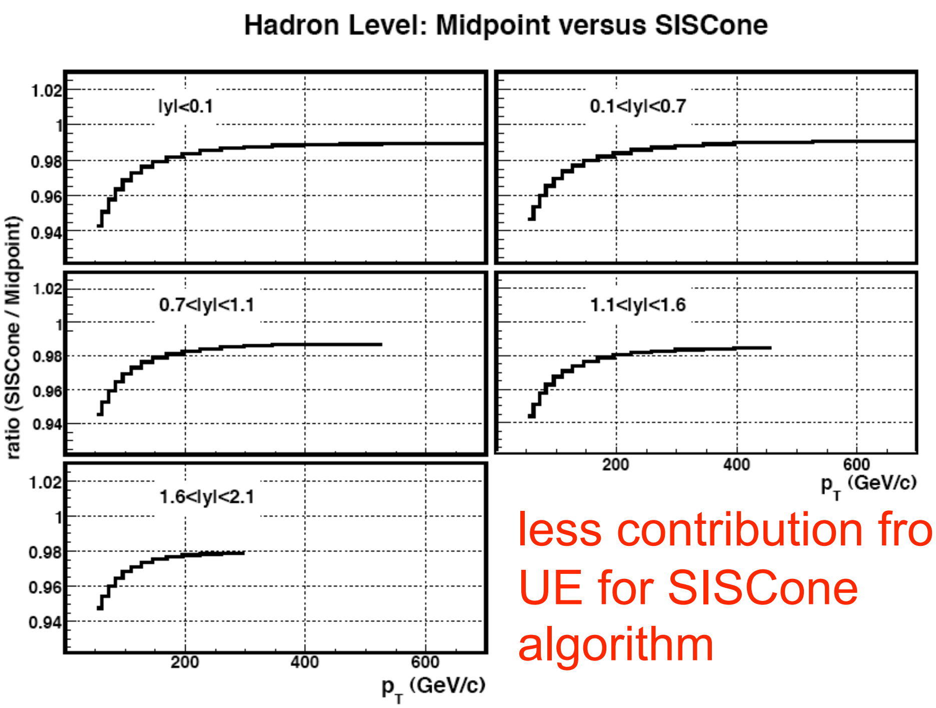

less contribution from UE for SISCone algorithm

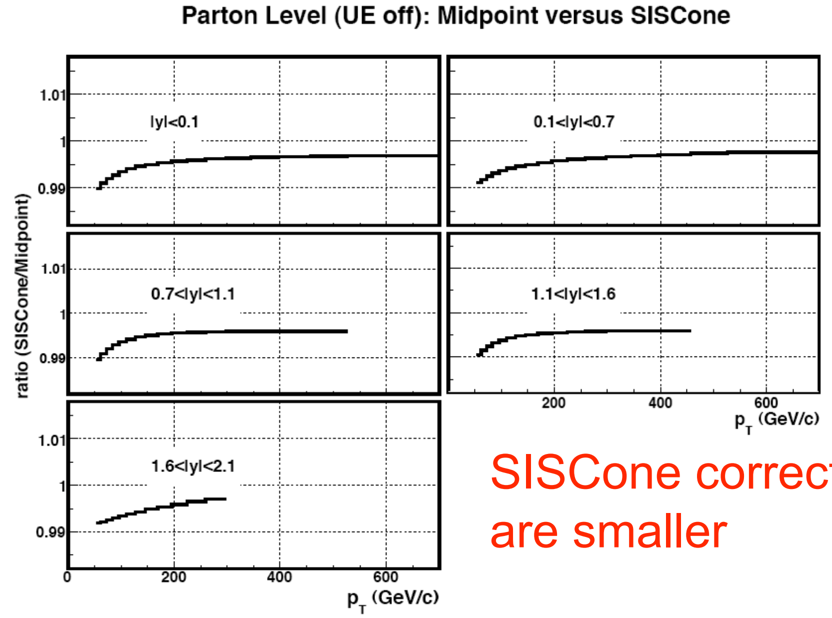

SISCone corrections are smaller

- So far, at the Tevatron, we have not explicitly measured a jet cross section using the SISCone algorithm, although studies are underway, but we have done some Monte Carlo comparisons for the inclusive cros sections
- Differences of the order of a few percent at the hadron level reduce to <1% at the parton level

New k_T family algorithms

- k_T algorithms are typically slow because speed goes as $O(N^3)$, where N is the number of inputs (towers, particles,…)
- Cacciari and Salam (hep-ph/0512210) have shown that complexity can be reduced and speed increased to O(N) by using information relating to geometric nearest neighbors
- Anti-k_T from Cacciari and Salam (reverse k_T: Pierre-Antoine Delsart) clusters soft particles with hard particles first
- Now the algorithm of choice for both ATLAS and CMS

$$d_{ij} = \min\left(p_{T,i}^{2p}, p_{T,j}^{2p}\right)\frac{\Delta R_{ij}^2}{D^2}$$

$$d_{ii} = p_{T,i}^{2p}$$

p=0; C-A
p=1: k_T
p=-1 anti-k_T

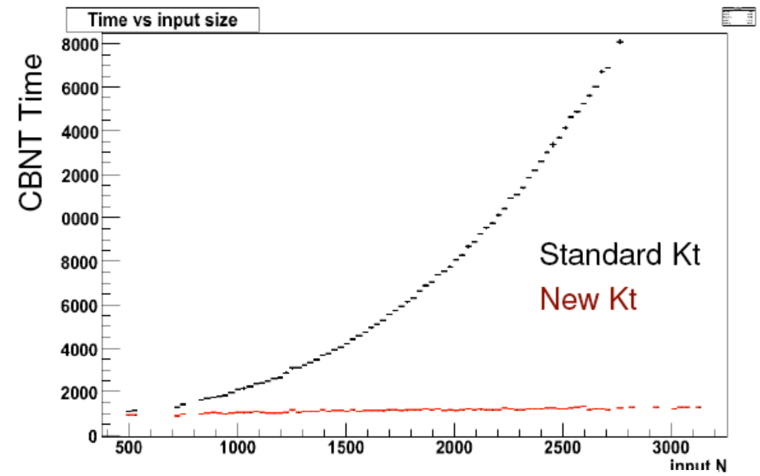

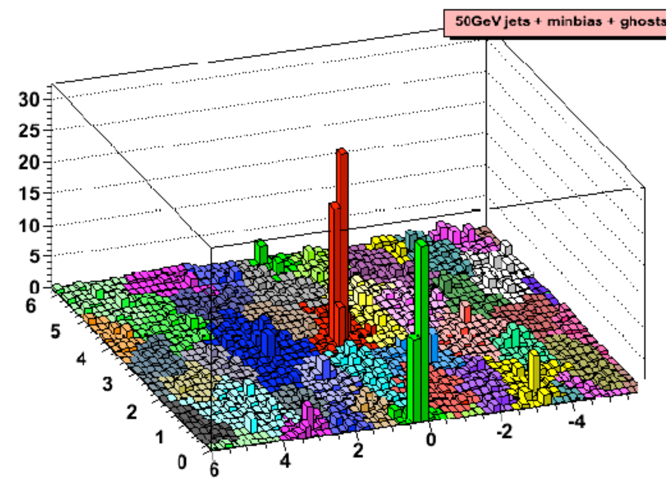

~ 10000 particles

Clustering takes ~ 20 minutes with old methods.

0.6s with FastJet.

Fragmentation functions

- On a more inclusive note, can define a fragmentation function $D(z,Q^2)$ that describes the probability to find a hadron of momentum fraction z (of the parent parton) at a scale Q
- The parton shower dynamically generates the fragmentation function, but the evolution of the fragmentation function with Q^2 can be calculated in pQCD (just as the evolution of the parton distribution functions can be calculated)
- But, like the PDFs, the value of $D(z,Q_o)$ is not known and must be determined by fits to data
- The data from LEP are the most useful for their determination

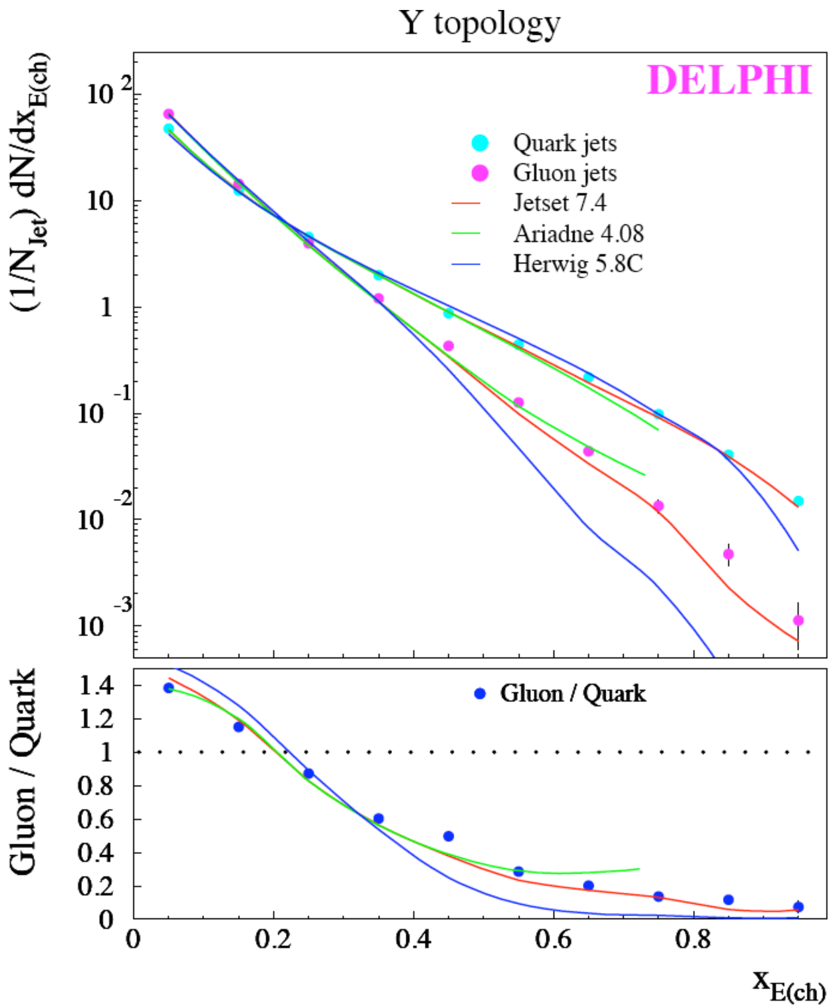

NB: the gluon fragmentation function is much softer; Herwig does not describe the high z gluon fragmentation function well

Some more details

- For outgoing quarks and gluons, have collinear singularities just as for the parton distribution functions
- Fragmentation functions acquire μ dependence just as PDFs did

$$\mu^2 \frac{\partial}{\partial \mu^2} D_i(x,\mu^2) = \sum_j \int_x^1 \frac{dz}{z} \frac{\alpha_s(\mu^2)}{2\pi} D_j\left(\frac{x}{z},\mu^2\right) P_{ji}\left(z,\alpha_s\left(\mu^2\right)\right)$$

- …just like DGLAP

Calculate single particle cross section by convoluting over fragmentation function

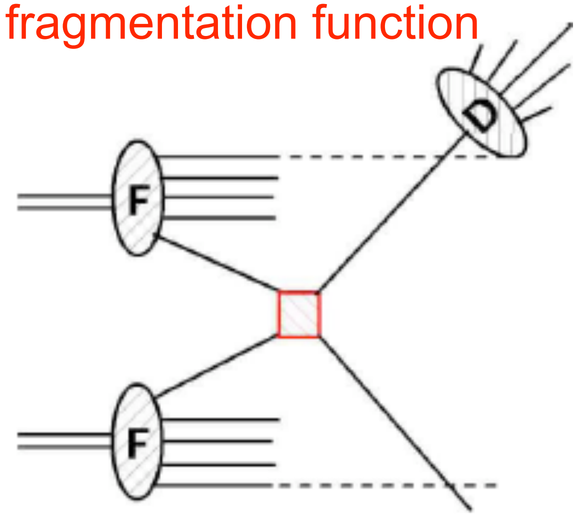

$$\frac{d\sigma_{pp}^{\pi}}{d\eta dp_T^2} = \iiint f_{a/p}\left(x_a,\mu_F\right) \otimes f_{b/p}\left(x_b,\mu_F\right) \otimes \hat{\sigma}_{ab\to c}\left(p_T,\frac{s}{p_T^2},x_1,x_2,z,\frac{p_T}{\mu_F},\frac{p_T}{\mu}\right) \otimes D_{\pi/c}\left(z,\mu_F\right) \times \left\{1 + \mathrm{O}\left(\frac{m^2}{p_T^2}\right)\right\}$$

- Lowest order splitting functions are identical to those discussed for PDFs

$$P_{ji}\left(z,\alpha_s\left(\mu^2\right)\right) = P_{ji}^{(0)} + \frac{\alpha_s\left(\mu^2\right)}{2\pi} P_{ji}^{(1)}(z) + \ldots$$

Sum over all fragmentation functions, apply a jet algorithm and voila you have a jet cross section

Photon production

- Production doesn't go out to as high a transverse momentum as for jets since the cross section is proportional to $\alpha\alpha_s$
- Photons can either be direct or from fragmentation processes
  - q->qγ
- There are backgrounds from jets which fragment into π^o's which contain most of the momentum (i.e. high z) of the original parton (quarks, not gluons)
- By imposing an isolation cut around the photon direction, the signal fraction can be greatly increased
- The isolation cut can either be a fraction of the photon transverse momentum, or a fixed cut
- To the right, the energy in the isolation cone is required to be less than 2 GeV (corrected for pileup)
  - this energy is dominated by the UE

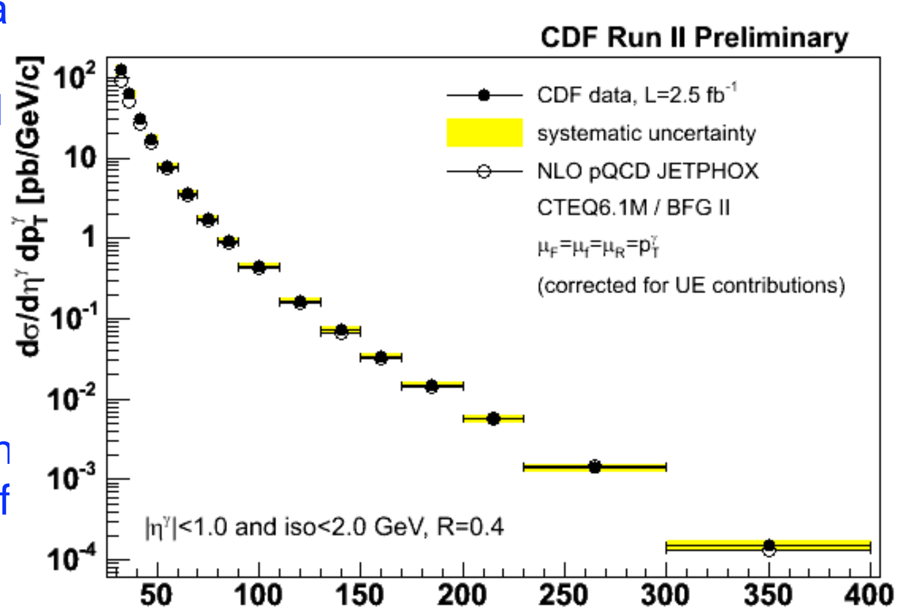

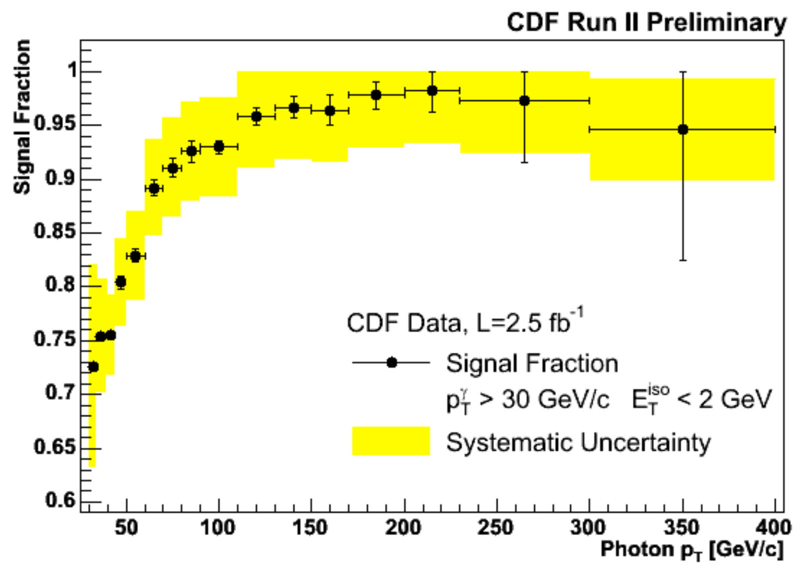

Comparison to NLO prediction

- Good agreement above 50 GeV/c
- Discrepancy below 50 GeV/c
- Also seen by D0 and by previous collider measurements of photon cross sections
- What gives?
- Remember the p_T of the W; here we had a two-scale problem (m_W and p_T^W); near p_T~0, the log was large and the effects of soft gluon radiation had to be resummed

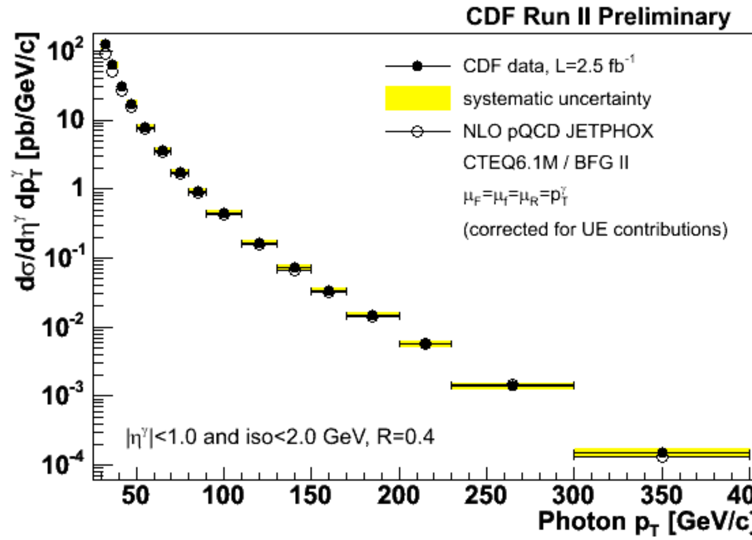

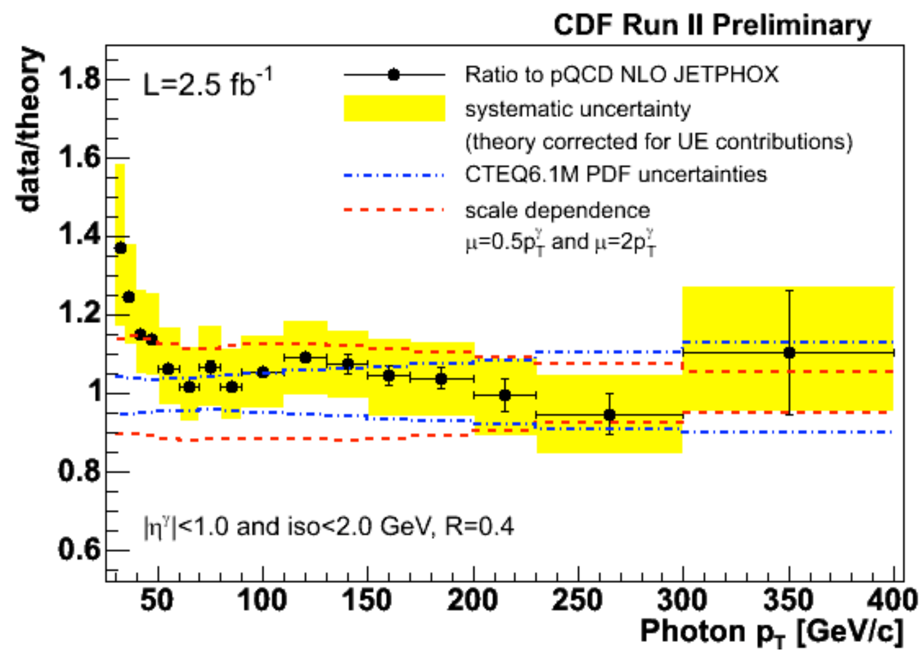

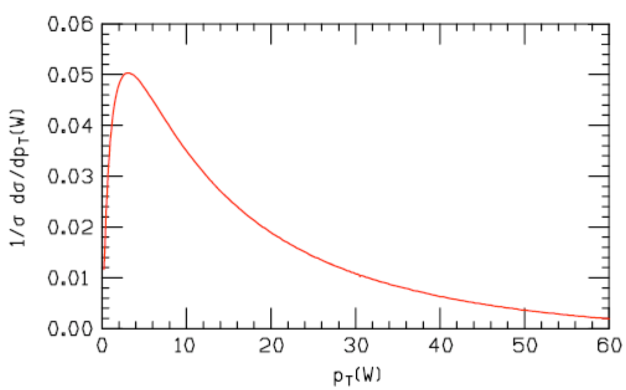

Figure 20. The resummed (leading log) *W* boson transverse momentum distribution.

k_T kick

- Here we only have 1 scale (p_T^γ) but fixed order pQCD does not seem to be doing well at low p_T
- Soft gluons are radiated by the incoming partons as they head towards the hard collision producing the photon
  - as we saw earlier that the PDF's have a Q^2 dependence because of this soft radiation
- They reduce the momentum fraction x carried by the parton but also give the parton a transverse momentum
- So that when the two partons collide, they have a relative transverse momentum
- This gives the photon a k_T kick, in a manner not described by fixed order pQCD

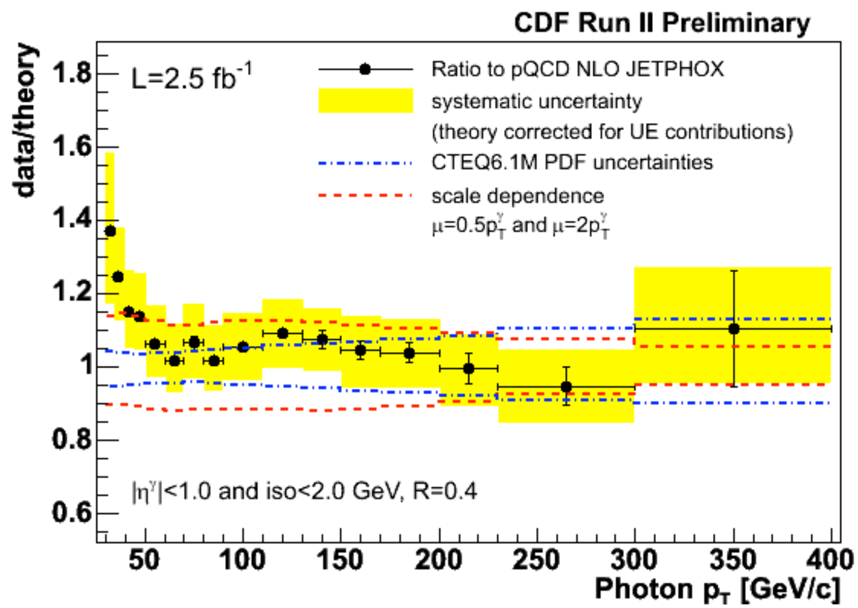

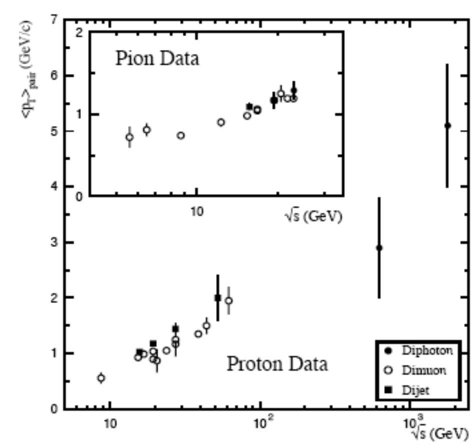

FIG. 1. $\langle p_T \rangle$ of pairs of muons, photons, and jets produced in hadronic collisions versus $\sqrt{s}$.

this kick gets larger as the center of mass increases (and as the mass of the final state increases)

k_T kick

- Since there aren't two scales can't use the normal q_T resummation formalism
- But can do a back-of-the envelope calculation

For definiteness, let us consider direct-photon production. The full 2-dimensional convolution of the (parametrized) differential cross section Σ (for example, $\Sigma = d\sigma/dp_T$) with the Gaussian k_T-smearing functions can be written as:

$$\Sigma'(p_T) = \int d^2k_{T_1} d^2k_{T_2} d^2q_T \, \frac{1}{\pi\langle k_{T_1}^2\rangle} e^{-k_{T_1}^2/\langle k_{T_1}^2\rangle} \, \frac{1}{\pi\langle k_{T_2}^2\rangle} e^{-k_{T_2}^2/\langle k_{T_2}^2\rangle}$$
$$\times \Sigma(q_T)\, \delta^{(2)}(\vec{p}_T - \vec{q}_T - \frac{1}{2}(\vec{k}_{T_1} + \vec{k}_{T_2})), \qquad (11)$$

A different representation, useful, for example, for parametrizing CDF and DØ measurements, assumes $\Sigma \sim 1/p_T^n$. For this parametrization (or more general functional forms) one can expand $\Sigma(p_T - k_T)$ as a power series in k_T (for k_T small compared to p_T):

$$\Sigma(p_T - k_T) = \Sigma(p_T) + \frac{1}{2!}k_T^2\Sigma''(p_T) + \frac{1}{4!}k_T^4\Sigma^{(4)}(p_T) + \ldots \qquad (16)$$

(the odd powers of k_T integrate out to zero). One obtains:

$$K(p_T) = 1 + \frac{\langle k_T\rangle^2}{2\pi}\frac{n(n+1)}{p_T^2} + \frac{\langle k_T\rangle^4}{8\pi^2}\frac{n(n+1)(n+2)(n+3)}{p_T^4} + \ldots \qquad (17)$$

For a constant (or a slowly changing) slope parameter n (and for $\langle k_T\rangle \ll p_T$), the effects of k_T smearing decrease as $1/p_T^2$, as might be expected for a power-suppressed process.

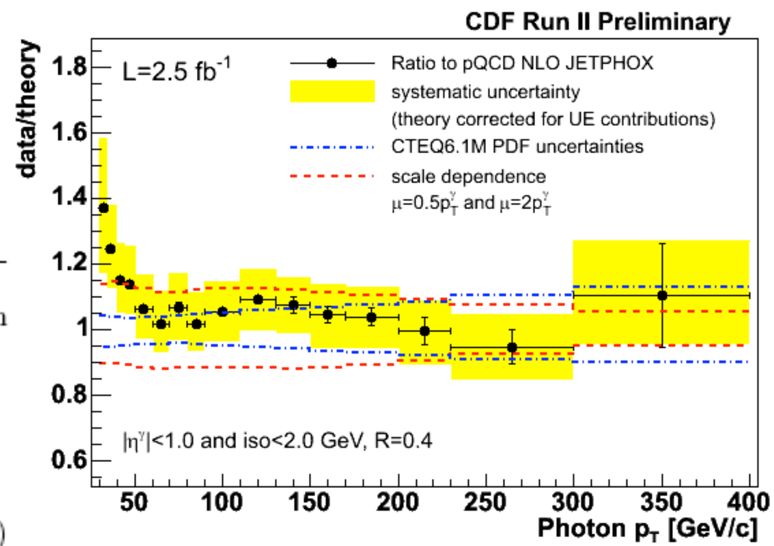

hep-ph/9808467

effect falls off by 50 GeV/c should be similar at LHC

in hep-ph/0002078, George Sterman and collaborators developed a formalism to handle this situation